*J Neurophysiol* 90: 739–754, 2003.
First published April 2, 2003; 10.1152/jn.00123.2003.

# Discharge Dynamics of Oculomotor Neural Integrator Neurons During Conjugate and Disjunctive Saccades and Fixation

**Pierre A. Sylvestre, Julia T. L. Choi, and Kathleen E. Cullen**
*Aerospace Medical Research Unit, Department of Physiology, McGill University, Montreal, Quebec H3G 1Y6, Canada*

Submitted 10 February 2003; accepted in final form 26 March 2003

**Sylvestre, Pierre A., Julia T. L. Choi, and Kathleen E. Cullen.** Discharge dynamics of oculomotor neural integrator neurons during conjugate and disjunctive saccades and fixation. *J Neurophysiol* 90: 739–754, 2003. First published April 2, 2003; 10.1152/jn.00123.2003. Burst-tonic (BT) neurons in the prepositus hypoglossi and adjacent medial vestibular nuclei are important elements of the neural integrator for horizontal eye movements. While the metrics of their discharges have been studied during conjugate saccades (where the eyes rotate with similar dynamics), their role during disjunctive saccades (where the eyes rotate with markedly different dynamics to account for differences in depths between saccadic targets) remains completely unexplored. In this report, we provide the first detailed quantification of the discharge dynamics of BT neurons during conjugate saccades, disjunctive saccades, and disjunctive fixation. We show that these neurons carry both significant eye position and eye velocity-related signals during conjugate saccades as well as smaller, yet important, "slide" and eye acceleration terms. Further, we demonstrate that a majority of BT neurons, during disjunctive fixation and disjunctive saccades, preferentially encode the position and the velocity of a single eye; only few BT neurons equally encode the movements of both eyes (i.e., have conjugate sensitivities). We argue that BT neurons in the nucleus prepositus hypoglossi/medial vestibular nucleus play an important role in the generation of unequal eye movements during disjunctive saccades, and carry appropriate information to shape the saccadic discharges of the abducens nucleus neurons to which they project.

## INTRODUCTION

The pioneering work of Robinson (1964) elegantly demonstrated that to generate saccades, motor commands proportional to the velocity of the eyes must be generated to overcome the viscous properties of the oculomotor plant. Furthermore, to keep the eyes at eccentric positions in the orbit, the brain must provide an additional and sustained motor command to the extraocular muscles to offset the restoring elastic forces of the oculomotor plant. When combined, these two motor commands would generate discharge patterns on motoneurons that are often referred to as "burst-tonic," or "pulse-step." It has been experimentally confirmed that burst-tonic signals are indeed carried by extraocular motoneurons during conjugate saccadic eye movements (Goldstein 1983; Keller 1973; Robinson 1970; Robinson and Keller 1972; Sylvestre and Cullen 1999a; Van Gisbergen et al. 1981). Conjugate saccades reorient the two visual axes between targets located at a same depth and produce equal amplitude rotations of the two eyeballs.

During conjugate saccades, there is general agreement that the "burst" discharge of brain stem saccadic burst neurons, which is roughly proportional to the velocity of the eyes (Cullen and Guitton 1997), is integrated (in the mathematical sense) to produce the eye-position command carried by motoneurons (reviewed in Scudder et al. 2002). This process is believed to occur through a distributed network known as the "oculomotor neural integrator" (NI). A number of studies (reviewed in Fukushima et al. 1992; McCrea 1988) have implicated the nucleus prepositus hypoglossi (NPH) and the adjacent medial vestibular nucleus (MVN) in the process of neural integration for horizontal eye movements. First, lesions made to these neural structures were shown to dramatically impair gaze-holding abilities (Arnold et al. 1999; Kaneko 1997; Mettens et al. 1994) and to a lesser extent perturb eye-movement dynamics (Kaneko 1997, 1999; Mettens et al. 1994). Second, it was shown that different classes of neurons that are distributed across the NPH/MVN have discharge properties consistent with those predicted for NI neurons. Among these types of neurons are burst-tonic (BT) and tonic (T) units (also termed burst-position and position neurons, respectively). These neurons all carry an eye-position-related signal (monkey: Cullen et al. 1993; McFarland and Fuchs 1992; Scudder and Fuchs 1992; cat: Delgado-Garcia et al. 1989; Escudero et al. 1992; Lopez-Barneo et al. 1982) and do not respond to vestibular stimulation during cancellation of the VOR (Cullen et al. 1993; McFarland and Fuchs 1992). Furthermore, in monkeys, the majority carry an eye-velocity-related signal during saccades that gives them BT discharge characteristics (Cullen et al. 1993; McFarland and Fuchs 1992; Scudder and Fuchs 1992). There is strong evidence that primate BT neurons project directly to the abducens nucleus (McFarland and Fuchs 1992; Scudder and Fuchs 1992).

The primary objective of this study was to determine the role of BT neurons in the binocular control of disjunctive saccades. These eye movements, which we frequently utilize to reorient our visual axes between targets located at different eccentricities and at different depths relative to our eyes, are characterized by the two eyes rotating by different angles and with markedly different dynamics. We also compare the signals carried by individual neurons during conjugate saccades, disjunctive saccades and fixation.

To date, the premotor control of binocular eye movements has been primarily studied during *nonsaccadic* disjunctive eye

Address for reprint requests: K. E. Cullen, McIntyre Medical Research Bldg, Rm 1220, 3655 Prom. Sir William Osler, Montreal, Quebec, H3G 1Y6, Canada (E-mail: kathleen.cullen@mcgill.ca).

The costs of publication of this article were defrayed in part by the payment of page charges. The article must therefore be hereby marked "*advertisement*" in accordance with 18 U.S.C. Section 1734 solely to indicate this fact.

movements. Most of these prior studies that have characterized the neurophysiology underlying the binocular control of eye movements (e.g., King and Zhou 2000; Mays 1998) have interpreted their results with respect to theoretical frameworks inspired by the original work of Hering (1868) and Helmholtz (1910). Simplified schemas illustrating the general concepts of each of these theories are shown in Fig. 1, *A* and *B*, respectively. The first schema (Fig. 1*A*) highlights that although the horizontal neural integrator is likely shared across many oculomotor behaviors, such as saccades, smooth pursuit, and the vestibuloocular reflex (reviewed by Fukushima et al. 1992; Moschovakis 1997), it should be exclusive to conjugate eye movements. In this view, a separate NI would exist for the vergence eye movements that ensure binocular alignment between targets located at different depths (e.g., Mays and Gamlin 1995a,b; Zee et al. 1992). A clear prediction of such a model structure is that NPH/MVN neurons are the substrate for a conjugate integrator, and therefore should solely encode the conjugate movements of the eyes (Fig. 1*A*) (Mays and Gamlin 1995, 1996).

There is experimental evidence that both supports and contradicts this concept. In support of this concept, a population of neurons in the mesencephalon, termed near-response neurons, have been identified that encode disparity and vergence position and velocity signals during symmetric vergence shifts (Mays 1984; Mays and Gamlin 1995a,b) and project to medial rectus motoneurons (Zhang et al. 1991, 1992). Vergence-velocity neurons, which are thought to project to near-response neurons, have also been identified (Mays et al. 1986; Mays and Gamlin 1995b). These neurons could form the vergence subsystem required in this schema. However, there is no evidence to date indicating that near-response neurons, or vergence-velocity neurons, project to lateral rectus motoneurons in the abducens nuclei (Fig. 1*A*, - - -) (Gamlin 1999). Moreover, other routes through which vergence-related signals could reach the abducens nuclei, for example via oculomotor internuclear neurons, have failed to demonstrate appropriate vergence modulations (Clendaniel and Mays 1994). Thus while near-response and vergence-velocity neurons most certainly play a role in shaping the discharge patterns of medial rectus motoneurons during vergence eye movements, their involvement in modulating the discharge patterns of abducens nucleus neurons (ABN) remains questionable. This is an important concern given that abducens nucleus neurons' firing rates are well modulated by vergence position and velocity-related signals during disjunctive fixation and disjunctive saccades (Sylvestre and Cullen 2002).

The second model structure, shown in Fig. 1*B*, is more consistent with Helmholtz's hypothesis (e.g., Zee et al. 1992; Zhou and King 1998 2000). Here, rather than using conjugate and vergence coordinates to control binocular movements (as in Fig. 1*A*), the brain utilizes right and left eye coordinates. Consequently, a prediction of this scheme is that neurons in the saccadic circuitry, including BT neurons, should be monocular. In agreement with this concept, it has been shown that BT neurons encode the position and velocity of a single eye during disjunctive smooth pursuit (Zhou and King 1996). Moreover, during disjunctive fixation, Chen-Huang and McCrea (1999) have noted that BT neurons in the MVN appear to preferentially encode the position of a single eye but provided no quantitative analysis of this observation. It should be noted, however, that there is strong experimental evidence from abducens neurons, during nonsaccadic disjunctive eye movements (Gamlin and Mays 1992; Gamlin et al. 1989; Keller 1973; Keller and Robinson 1972; King et al. 1994; Mays and Porter 1984; Sylvestre and Cullen 2002; Zhou and King 1996, 1998), which indicate that this model's predictions clearly do not hold. Specifically, it has been shown that abducens internuclear neurons and motoneurons encode similar signals during disjunctive eye movements (Fig. 1*B*). Finally, this model would offer no explanation for the existence of near-response and vergence-velocity neurons.

Most recently, a very limited number of studies have begun to address which of these model structures best describes the

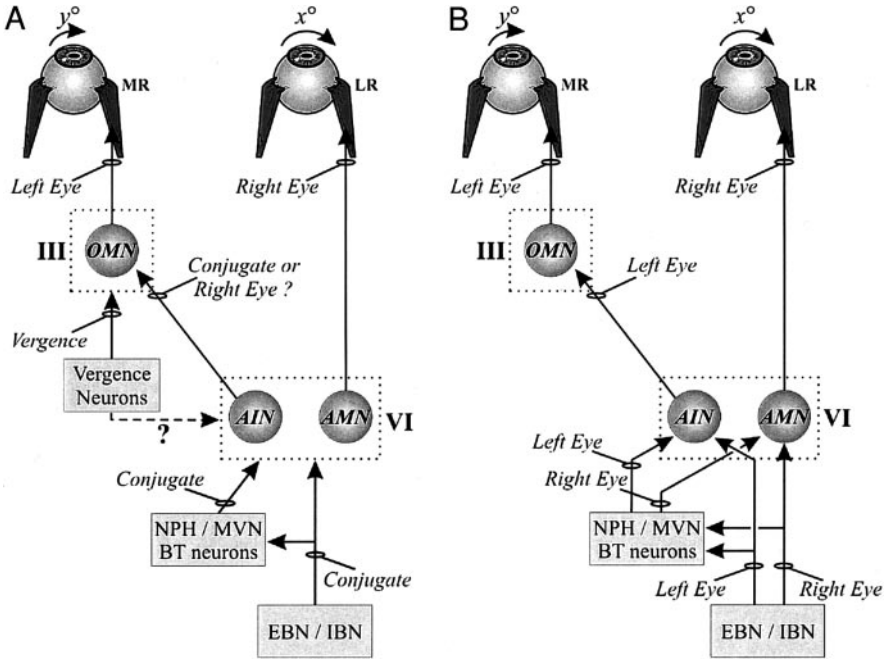


FIG. 1. Theoretical frameworks of binocular control. *A*: in this 1st scheme, which was inspired from the theory of Hering, burst-tonic (BT) neurons encode the conjugate position of the eyes. A vergence signal is provided to both the abducens (VIth) and the oculomotor (IIIrd) nuclei by vergence neurons. *B*: in this second scheme, that was inspired from the theory of Helmholtz, BT neurons encode signals that are either related to the movements of the right or of the left eye. Vergence neurons are not utilized in this theory. MR, medial rectus; LR, lateral rectus; OMN, oculomotor motoneuron; AIN, abducens internuclear neuron; AMN, abducens motoneuron; EBN/IBN, excitatory and inhibitory burst neurons.

premotor control of disjunctive saccades. On the one hand, we have reported that the discharge dynamics of all abducens neurons are similar during disjunctive saccades, implying that motoneurons and internuclear neurons do not carry different information (Sylvestre and Cullen 2002). Thus as during non-saccadic disjunctive eye movements, experimental data are not completely consistent with the predictions of the model structure shown in Fig. 1*B*. On the other hand, it has been shown that the number of spikes generated by excitatory burst neurons (EBNs) are generally related to the displacement of a single eye (Zhou and King 1998). Thus it has been argued that EBNs encode monocular signals, consistent with Fig. 1*B*. Given that EBNs provide a significant drive to BT neurons during disjunctive saccades, these results suggest that BT neurons would also encode disjunctive signals during this behavior. In the present study, we test this prediction.

Taken together, the results from prior single-unit recording experiments cannot be accurately represented by either of these straightforward conceptual frameworks. Accordingly, more physiologically realistic frameworks have been proposed (Cova and Galiana 1994–1996; King and Zhou 2000, 2002; Sylvestre et al. 2002). These more recent models have in common that abducens internuclear neurons and motoneurons encode similar signals, near-response neurons project to oculomotor motoneurons but not to abducens neurons, the vergence signals carried by near-response neurons correct for the "inappropriate" signals carried by abducens internuclear neurons, and the activity of near-response neurons is shaped by bilateral projections from monocular NI neurons. The main difference among these models is that during disjunctive saccades, the Cova and Galiana (1996; see also Sylvestre et al. 2002) model includes that premotor neurons encode the movements of the ipsilateral eye, whereas in the King and Zhou (2000, 2002) model, brain stem premotor neurons are organized in two separate channels, one for each eye.

In the present study, we demonstrate that neither of the conceptual frameworks presented in Fig. 1, *A* and *B*, can fully account for the population discharges of BT neurons during disjunctive saccades and fixation. For each BT neuron we recorded, our analysis approach first involved quantifying its discharge dynamics during the simpler case of conjugate saccades. Then during disjunctive saccades, we determined whether the activity patterns of that neuron could be predicted based on its discharge dynamics during conjugate saccades. We also directly quantified the discharge dynamics of this same neuron during disjunctive saccades using a model that accounted separately for the movements of both eyes. We argue in DISCUSSION that our data are more consistent with the predictions of the more recent models by Cova and Galiana (1994–1996) and King and Zhou (2000, 2002).

## METHODS

Three rhesus monkeys (*Macaca mulatta*) were prepared for chronic extracellular recording using the aseptic surgical procedures described previously (Sylvestre and Cullen 1999a). A stainless steel post that allowed the complete immobilization of the animal's head and two stainless steel recording chambers oriented stereotaxically toward the right and left abducens nuclei, respectively, were fastened to the animal's skull using cranial screws and dental acrylic. An eye coil (3 loops of Teflon-coated stainless steel wire, 18- to 19-mm diam) was implanted in each eye (Judge et al. 1980). All procedures were approved by the McGill University Animal Care Committee and were in compliance with the guidelines of the Canadian Council on Animal Care.

### *Data-acquisition procedures*

During the experiment, the head-restrained monkey was seated in a primate chair that rested on a vestibular turntable. Targets, rewards, on-line data displays, and data acquisition were controlled on-line using REX (Real-Time Experimentation System) (Hayes et al. 1982). When a neuron was properly isolated, its activity was recorded on a digital audio tape together with the horizontal and vertical positions of the right and left eyes, the velocity of the vestibular turntable and the position of the target. Off-line analysis was performed using custom algorithms (Matlab, The MathWorks).

The magnetic search-coil technique was utilized to record the horizontal and vertical positions of both eyes (Fuchs and Robinson 1966) (CNC Engineering). Each eye coil signal was calibrated independently by having the monkey fixate monocularly (i.e., 1 eye masked) on a variety of targets at different eccentricities and depths. Note that only eye movements restricted to the horizontal plane are discussed in the present report. Off-line, right eye, left eye and target position signals were first low-pass filtered at 250 Hz (analog 8 pole Bessel filter) and sampled at 1 kHz. Recorded eye position signals were next digitally filtered with a 51st-order finite-impulse-response (FIR) filter with a Hamming window, using a cut-off at 125 Hz. The position signals were differentiated to produce eye velocity profiles. Zero-phase forward and reverse digital filtering prevented phase distortion.

Extracellular single-unit activity was recorded using enamel-insulated tungsten microelectrodes (7- to 10-M$\Omega$ impedance, Frederick Haer). A neuron was considered to be adequately isolated only when, on playback, individual action potential waveforms could be discriminated during saccades, smooth pursuit, and fixation, using a windowing circuit (BAK) (for example, see Fig. 1 in Sylvestre and Cullen 1999a). Neuronal discharges were represented as a spike density function in which a Gaussian function (SD of 5 ms for saccades, and 10 ms for smooth pursuit, cancellation of the VOR, and fixation) was convolved with the spike train (Cullen and Guitton 1997; Cullen et al. 1996; Sylvestre and Cullen 1999a,b, 2002).

To determine the location of the nucleus prepositus, the location of the abducens nucleus was first identified based on its stereotypical discharge patterns during eye movements (Cullen et al. 1993; Sylvestre and Cullen 1999a). Previous studies had shown that burst tonic neurons are distributed between the vestibular nuclei and nucleus prepositus hypoglossi (Cullen at al. 1993; McFarland and Fuchs 1992). In the present study, single-unit recordings were for the most part limited to a small region of the brain stem extending 0.5–1.5 mm caudal to the abducens nucleus and 0.5–1.5 mm lateral of the midline, corresponding to the nucleus prepositus (Brodal 1983; McCrea et al. 1987). Reconstructions of recording locations indicated that most neurons (85%) were located within this area. The remaining small percentage of neurons (15%) were located in the most rostromedial aspect of the adjacent rostral-medial vestibular nucleus. Note that in addition to these anatomical criteria, we were careful to prevent, as much as possible, the inclusion of abducens neurons in our sample by restricting our analysis to BT neurons for which no BT activity could be recorded in the background (i.e., no "beehive" sound characteristic of the abducens nucleus) (see Robinson 1970; Sylvestre and Cullen 1999a, 2002) or in the neuron's immediate vicinity.

### *Behavioral paradigms*

Monkeys were trained to fixate a target light in a dimly lit room for a juice reward. The paradigms utilized in the present study were identical to those used by Sylvestre and Cullen (2002).

CONJUGATE PARADIGMS. A red HeNe laser target projected onto a cylindrical screen located 55 cm away from the monkey's eyes (isovergent, ~3.5° convergence) was utilized for all conjugate paradigms. To elicit saccades, the target light was stepped between positions ±5–30°, in 5° increments and in predictable or nonpredictable sequences. Fixation intervals were obtained by keeping the target stationary for 2–3 s at each position. Smooth pursuit eye movements were generated by moving the same laser target sinusoidally (40°/s peak velocity, 0.5 Hz). Cancellation of the vestibuloocular reflex (VORc) was also utilized to verify that neurons were not sensitive to vestibular stimulation. In this paradigm, the monkey fixated a laser target that moved with the primate chair during sinusoidal whole-body rotations (40°/s peak velocity, 0.5 Hz).

DISJUNCTIVE PARADIGMS. We utilized an array of 16 computer-controlled red light-emitting diodes (LEDs; with intensities comparable to that of the laser target) placed between the cylindrical screen and the monkey's eyes to elicit vergence eye movements. First, symmetric (pure) vergence eye movements were obtained using targets that were aligned with the monkey's midsaggital plane (convergence angles: LEDs: 17, 12, 8, and 6° and laser: 3.5°). Second, disjunctive saccades were generated by stepping the target from one of the 16 LEDs to one of the eccentric laser target positions (described in the preceding text for saccades). Predictable and nonpredictable target sequences were utilized (see Sylvestre and Cullen 2002 for details). This approach yielded a rich variety of disjunctive saccades with conjugate components of amplitudes ±5–30° and vergence components of amplitudes ±4–13°.

### *Data analysis*

In this report, the eyes are referred to as either ipsilateral or contralateral based on their location relative to the recording site. For both the ipsilateral and contralateral eye, positive and negative values correspond to positions right and left of the mid-saggital plane, respectively. We also describe eye movements in terms of conjugate {conjugate = (left eye + right eye)/2} and vergence (vergence = left eye − right eye) coordinates.

CONJUGATE AND DISJUNCTIVE FIXATION. A neuron's sensitivity to eye position during conjugate fixation was measured as the slope of the relationship between the mean conjugate eye position and mean firing rate measured during such intervals. Conjugate fixation periods ($n > 40$) were defined as time intervals ≥200 ms in duration, during which the vergence angle was <3.5° and the peak conjugate and vergence velocities were <10°/s. To avoid fitting neuronal response as cells were driven into cut-off, only data for which the firing rate was >20 spikes/s were included in the optimization. A similar analysis was performed during disjunctive fixation (defined as having vergence angle > 4°; $n > 40$ segments) using a multiple regression model that included the mean position of each eye. Standard statistical tests were performed on the model parameters to determine 95% confidence intervals.

CONJUGATE SACCADES. The dynamic sensitivity of a neuron to eye movements during conjugate saccades ($n > 40$) was estimated using linear optimization techniques that have been described in detail elsewhere (Sylvestre and Cullen 1999a). By definition, horizontal conjugate saccades had vertical amplitudes <10% of their horizontal amplitudes, and changes in vergence angles <2.5°. The onset and offset of these saccades was determined using a typical 20°/s velocity criterion. The specific model structures utilized are described in Table 2. The goodness-of-fit to the data of each model was quantified using the variance-accounted-for {VAF = 1 − [var(mod − fr)/var(fr)], where mod represents the modeled firing rate and fr represents the actual firing rate}. The VAF is equivalent to the $R^2$ coefficient for linear models and can be easily utilized to evaluate the goodness-of-fit of model predictions. A Bayesian Information Criteria (BIC) was also computed for each model (Cullen et al. 1996). This criteria serves as a "cost index" that indicates whether increasing the complexity of the model is justified by the accompanying increase in VAF (Schwartz 1978). The dynamic lead time of individual neurons ($t_d$) was determined during conjugate saccades as described in Sylvestre and Cullen (1999a).

DISJUNCTIVE SACCADES. The activity of BT neurons during disjunctive saccades was first quantified using model *Est-all*, and then using model *Est-cv* (see RESULTS). The analysis of neuronal responses was limited to the saccadic interval. Note that ~80% of the vergence shift is executed during this interval for disjunctive saccades like those utilized here, for which the conjugate component is larger than the vergence component (see Maxwell and King 1992). Specifically, the analysis utilized disjunctive saccades during which both eyes moved in the same direction to limit the analysis to ON-direction responses only, one eye moved more than the other to generate vergence velocities >100°/s (mean intra-saccadic vergence shift: 6.5 ± 1.1°), and the onset and offset were marked using a 20°/s conjugate velocity criterion. Similar to our previous study of ABN neurons (Sylvestre and Cullen 2002), we estimated the probability distribution of the model parameters in *Est-all* (or *Est-cv*) using a nonparametric bootstrap approach (Carpenter and Bithell 2000; Press et al. 1997; Richmond et al. 1987; Sokal and Rohlf 1995). Briefly, for each neuron 1999 "new data sets" of $n > 40$ saccades were obtained by randomly re-sampling with replacement from an original data set (with $N/2$ converging saccades and $N/2$ diverging saccades; such balance is important to avoid biasing the parameter estimates). The model parameters were then estimated on each of the new data sets. The 1999 parameter values obtained with this approach were then utilized to compute 95% confidence intervals (BCa method) (Carpenter and Bithell 2000). Parameters with 95% confidence intervals that overlapped with zero were not statistically significant, and parameters with 95% confidence intervals that overlapped with one another were statistically identical. To prevent the biasing of meaningful parameter values due to the inclusion of inappropriate parameters in the original model, these inappropriate parameters were removed (if nonsignificant) or replaced (if identical) one at a time from the original model, and the parameters of the reduced model were estimated after each removal.

For each neuron, $Ratio_{fix}$ (for the eye position sensitivities during fixation), $Ratio_{pos}$ (for the eye position sensitivities during disjunctive saccades) and $Ratio_{vel}$ (for the eye velocity sensitivities during disjunctive saccades) indexes were computed using the reduced binocular model parameters (*Est-red*, see RESULTS) to quantify a unit's relative preference for one eye versus the other. For each sensitivity, a ratio index was computed using Ratio = [smaller parameter value]/[larger parameter value], where the smaller and larger parameter values are yielded by the nonpreferred and preferred eyes, respectively. To indicate which eye provided the larger parameter value (i.e., the neuron's "preferred eye"), each Ratio index was assigned an "i" or a "c", for the ipsilateral or contralateral eye, respectively. Using their ratio indexes, neurons were assigned to one of five categories based the criteria described in Table 1.

## RESULTS

The neurons included in this report were all responsive to horizontal eye movements and unresponsive to passively applied head movements during VORc. All neurons (20/20) had a clear horizontal eye position sensitivity during fixation with 90% increasing their discharge for increasingly eccentric ipsilateral eye positions (re. recording site). All but one neuron also had an horizontal eye-velocity sensitivity during saccades. Hence most neurons described in this report correspond to the BT type previously described (Cullen et al. 1993; McFarland and Fuchs 1992; Scudder and Fuchs 1992). In the following

TABLE 1. *Categories of ocular preferences*

| Category | Criteria | Ratio Value | Subscript |
|---|---|---|---|
| Mono. ipsi. | Contra. eye par. = 0<br>Ipsi. eye par. ≠ 0 | 0 | i |
| Mono. contra. | Ipsi. eye par. = 0<br>Contra. eye par. ≠ 0 | 0 | c |
| Bino. ipsi. | Ipsi. eye par. > Contra. eye par.<br>Ipsi. eye par. ≠ Contra. eye par. ≠ 0 | $-1 \leq$ Ratio $< 1$, Ratio $\neq 0$ | i |
| Bino. contra. | Ipsi. eye par. < Contra. eye par.<br>Ipsi. eye par. ≠ Contra. eye par. ≠ 0 | $-1 \leq$ Ratio $< 1$, Ratio $\neq 0$ | c |
| Conj. | Ipsi. eye par. = Contra. eye par.<br>Ipsi. eye par. ≠ Contra. eye par. ≠ 0 | 1 | |

Mono, monocular; Bino, unequal binocular; Conj, conjugate (i.e. equal binocular); Ipsi, ipsilateral eye preference; Contra, contralateral eye preference; Par, parameter value.

sections, we first describe the discharge properties of the recorded neurons during conjugate and disjunctive fixation. We next provide the first quantitative description of the discharge dynamics of BT neurons during conjugate saccades. After this characterization, we demonstrate our analysis approach of the discharge dynamics of the same neurons during disjunctive saccades using two example neurons. Finally, we present the distribution of discharge properties measured during disjunctive saccades across our sample of neurons.

### *Conjugate and disjunctive fixation*

The eye-position sensitivities of BT neurons were first evaluated during conjugate fixation intervals. In agreement with previous studies (Cullen et al. 1993; McFarland and Fuchs 1992), all neurons significantly encoded the position of the eyes in the orbit. The firing rate of two example units (*units B61_2* and *B43_1*) during intervals of conjugate fixation are shown in Fig. 2, *A* and *B* (■). Eye position traces are illustrated below (see legend). Each neuron's eye position sensitivity was quantified using a standard model ($\overline{FR} = b_{fix} + k_{fix}\overline{CJ}$, where $b_{fix}$ and $k_{fix}$ are the bias and eye position sensitivity coefficients, respectively, and $\overline{FR}$ and $\overline{CJ}$ are mean firing rate and conjugate eye position, respectively). This simple model provided good fits to the data (VAF = 0.71 ± 0.20, mean ± SD). The average $b_{fix}$ for our sample was 66 ± 48 spikes/s, and the average $k_{fix}$ was 3.2 ± 2.0 spikes · $s^{-1}$ · $^{\circ -1}$.

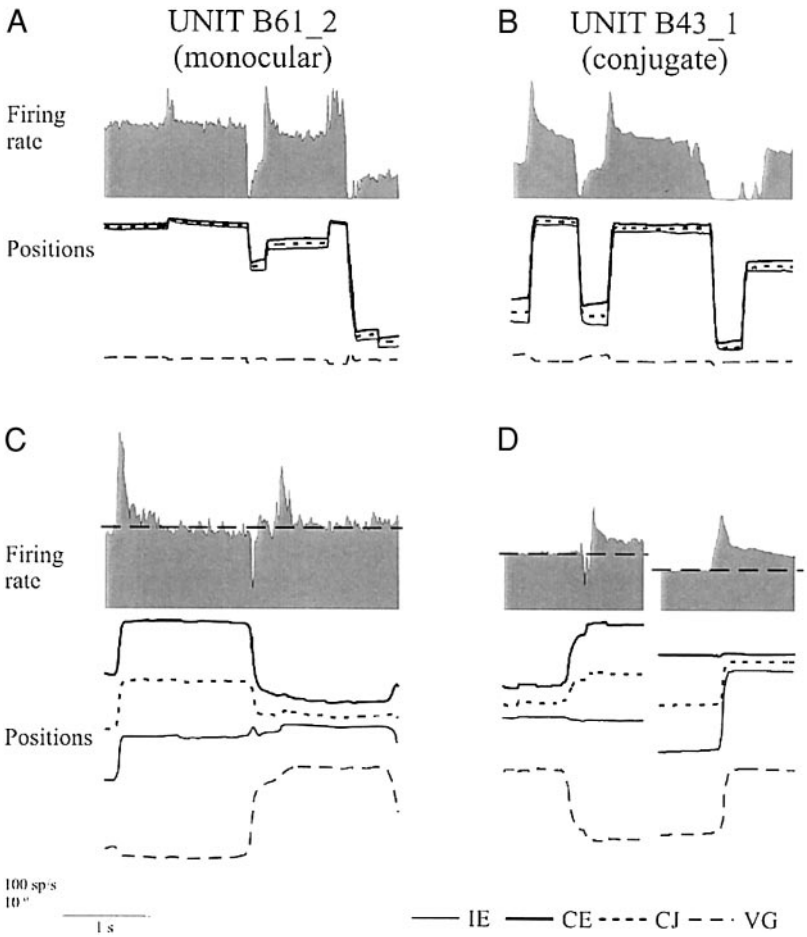


FIG. 2. Two example BT neurons during steady fixation. Both *unit B61_2* (*A*) and *unit B43_1* (*B*) had discharges that were modulated by the position of the eyes in the orbit during periods of conjugate fixation. The gray shaded areas represent the neurons's firing rates. Other traces are conjugate (CJ), vergence (VG), ipsilateral (IE), and contralateral (CE; re recording site) eye positions (see legend). Upward is in the direction ipsilateral to the recording site. *C*: during disjunctive fixation, *unit B61_2* encoded the position of the ipsilateral eye only. - - -, highlight that when the ipsilateral eye was kept at a relatively constant position, but the contralateral eye fixated at different positions, the neuron's firing rate was not modulated. *D*: in contrast, *unit B43_1* encoded the conjugate position of the eyes. During the same protocol, this neuron's activity was clearly modulated when the position of the contralateral eye changed but that of the ipsilateral eye did not (*left*) and also in the opposite condition when the position of the ipsilateral eye changed and that of the contralateral eye was kept constant (*right*).

During disjunctive fixation, most units' firing rates were modulated differentially by the position of each eye. This is clearly seen in Fig. 2*C*, where *unit B61_2*'s discharges were not modulated when the position of the ipsilateral eye (re the recording site) was kept relatively constant but the position of the contralateral eye was changed markedly. Hence this unit appeared to only encode the position of the ipsilateral eye. In contrast, other neurons' firing rates, like those of *unit B43_1*, were modulated by the position of both eyes (Fig. 2*D*). Clearly, this neuron's discharges were modulated even when the position of one of the eyes, or that of the other eye, was kept constant. Because this neuron obviously encoded the position of both eyes, possibly with different sensitivities, a more detailed quantitative analysis was warranted. In this case, as shown below, the quantitative analysis of this neuron's discharges has revealed that it was equally sensitive to the position of both eyes (i.e., it encoded the conjugate position of the eyes).

We quantified this observation using a rich data set of disjunctive fixation intervals (see METHODS) and a second model that included separate terms to estimate a neuron's sensitivity to the position of each eye ($\overline{FR} = b_{fix} + k_{i\text{-}fix}\overline{IE} + k_{c\text{-}fix}\overline{CE}$, where IE and CE represent the ipsilateral and contralateral eyes, respectively). This model also provided good fits to the data for our sample of neurons (mean VAF = 0.72 ± 0.19). For the example neuron shown in Fig. 2, *A* and *C*, the model parameter $k_{i\text{-}fix}$ was 3.47 spikes · $s^1$ · $°^{-1}$ and the parameter $k_{c\text{-}fix}$ was not significantly different from zero ($P > 0.05$), indicating that this neuron only encoded the position of the ipsilateral eye. In contrast, for the example neuron shown in Fig. 2, *B* and *D*, the model parameters $k_{i\text{-}fix}$ and $k_{c\text{-}fix}$ were statistically identical (1.6 spikes · $s^1$ · $°^{-1}$; $P > 0.05$), suggesting that this neuron equally encoded the position of both eyes (i.e., encoded the conjugate position of the eyes). Hence the analysis results confirmed the qualitative observations made in the preceding text for both neurons.

On average, across our sample of neurons, $k_{i\text{-}fix}$ was 0.9 ± 2.9 spikes · $s^1$ · $°^{-1}$, and $k_{c\text{-}fix}$ was 1.8 ± 2.4 spikes · $s^1$ · $°^{-1}$. To better describe the signals encoded by BT neurons during disjunctive fixation at the sample level, we quantified the relative preference of a neuron for one eye versus the other by computing a $Ratio_{fix}$ index for (see METHODS). This index was used to assign each neuron in our sample to one of five categories based the criteria described in Table 1: a neuron could be monocular with a preference for the ipsilateral eye, monocular with a preference for the contralateral eye, unequal binocular with a preference for the ipsilateral eye, unequal binocular with a preference for the contralateral eye, or conjugate (i.e., equal binocular sensitivities). Figure 3 shows the distribution of BT neurons, with respect to their eye position sensitivities during disjunctive fixation, obtained using this classification. Note that each category was assigned a different color (see legend). As shown in Fig. 3, an important fraction of BT neurons (40%) were monocular (gray bars), with roughly equal number of neurons preferring the ipsilateral (pale gray bar) or the contralateral (dark gray bar) eye. Most of the remaining neurons unequally encoded the binocular position of the eyes (stripped bars), with a slight preference for the contralateral eye. Only few neurons (20%) equally encoded the position of both eyes (i.e., were conjugate, black bar). We conclude that most BT neurons (80%) differently encode right and left eye position signals during disjunctive fixation.

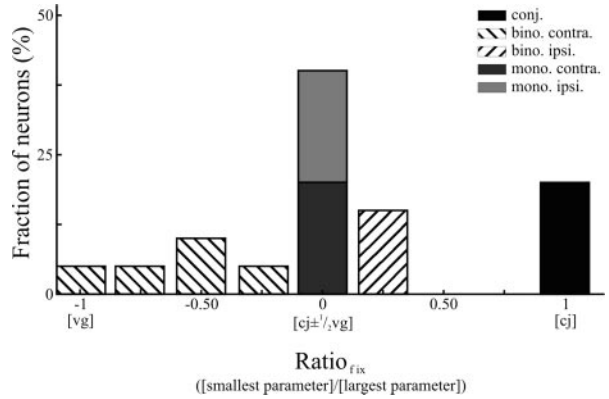


FIG. 3. Distribution of $Ratio_{fix}$ during disjunctive fixation for our sample of BT neurons. Axis labels between square brackets represent the alternative conjugate/vergence coordinate system.

These results can also be interpreted in the conjugate/vergence coordinate system. From the definitions of conjugate and vergence (see METHODS), it can be derived that

$$k_{conjugate} = k_{left\ eye} + k_{right\ eye}$$

$$k_{vergence} = (k_{left\ eye} - k_{right\ eye})/2$$

It follows that only those neurons that equally encode the position of the right and left eyes (e.g., *unit B43_1*, where $k_{left\ eye} = k_{right\ eye}$) have no vergence sensitivities. Because only 20% of the neurons in our sample matched this criteria, we conclude that the majority (i.e., 80%) of BT neurons in our sample encoded both vergence *and* conjugate position signals during disjunctive fixation.

### *Conjugate saccades*

Before quantifying the discharge patterns of BT neurons during disjunctive saccades, we determined, for the first time, what signals are carried by these neurons during the simpler situation of conjugate saccades (where both eyes rotate in the same direction, by the same amplitude, and with very similar dynamics). To do so, the goodness-of-fit of the different eye movement-based models shown in Table 2 were compared to determine which one provided the most appropriate description of BT neuron discharges during these eye movements. Note that we tested an extensive series of model structures on our sample of BT neurons but that for the sake of simplicity, only the most relevant models are reported in Table 2. Model fits obtained with three of the models in Table 2 are illustrated in Fig. 4 for two example BT neurons, u*nits B87_1* (*A*) and *B43_1* (*B*). For each neuron, three conjugate saccades of increasing amplitudes are shown. For clarity, the neurons' firing rates during these saccades are replicated three times (gray shaded curves, *top 3 rows*), and a different model fit (thick black curve) is shown in each row. Note that both units had clear bursts during conjugate saccades.

The first model we tested was solely based on a bias term (the firing rate when the monkey was fixating straight ahead) and the conjugate position of the eyes in the orbit (model M1, Table 2). This model provided a poor fit to the data (see *top row*, Fig. 4; mean VAF = 0.24 ± 0.25, Table 2). A second model, which was

TABLE 2. *Downstream models and mean VAF and mean BIC values estimated during saccades*

| | Models | *n* | $\overline{\text{VAF}}$ | $\overline{\text{BIC}}$ | $\Delta\ \overline{\text{VAF}}$ |
|---|---|---|---|---|---|
| M1 | $\text{FR}(t) = b + kE(t - t_d)$ | 2 | 0.24 ± 0.25 | 8.1 ± 1.3 | −0.32 |
| M2 | $\text{FR}(t) = b + r\dot{E}(t - t_d)$ | 2 | 0.28 ± 0.26 | 8.1 ± 0.84 | −0.28 |
| M3 | $\text{FR}(t) = b + kE(t - t_d) + r\dot{E}(t - t_d)$ | 3 | 0.56 ± 0.25 | 7.5 ± 1.1 | — |
| M4 | $\text{FR}(t) = b + kE(t - t_d) + r\dot{E}(t - t_d) + u\ddot{E}(t - t_d) - c\dot{\text{FR}}$ | 5 | 0.68 ± 0.19 | 7.2 ± 1.1 | 0.12 |

Values are ± SD. *n* = number of model parameters; $\Delta\ \overline{\text{VAF}}$, calculated relative to model M3. VAF, variance-accounted-for model; BIC, Bayesian Information Criteria.

based on a bias term and the conjugate velocity of the eyes, only marginally improved our ability to describe the neuronal discharges (model M2; mean VAF = 0.28 ± 0.26, Table 2; not shown in Fig. 4).

The simplest model that provided a good description of BT neuron discharges during conjugate saccades contained *both* eye position- and eye-velocity-related terms (model M3, Table 2; *2nd row*, Fig. 4). The average VAF values generated with this model were virtually twice larger than those obtained with the two simpler models (133 and 100% relative improvements, model M1 and M2, respectively). This striking increase in goodness-of-fit can be visualized by comparing the model fits shown in the *first* and *second rows* of Fig. 4. The average *b* coefficient for this model was 143 ± 82 spikes/s, the average *k* was 3.9 ± 2.5 spikes · $s^1$ · $°^{-1}$, and the average *r* was 0.34 ± 0.31 spikes/°. When compared with fixation, the bias coefficients were significantly larger during saccades ($P < 0.01$, paired *t*-test), but the *k* coefficients were not statistically different ($P > 0.05$). Models that included higher-order derivatives of eye position (e.g., eye acceleration and jerk) generally did not better describe the activity of BT neurons than model M3 (not shown). One exception was when a term proportional to the derivative of the firing rate (a "slide" term) was added to model M3 together with an eye acceleration term (model M4, Table 2; *3rd row*, Fig. 4); these terms provided an important increase in VAF across our sample of neurons (21% mean improvement relative to model M3). On average, the *u* coefficient (0.002 ± 0.005 spikes · $s^{-1}$ · $°^{-1}$) and the *c* coefficients (0.018 ± 0.018) were small. Hence, as for neurons in the abducens nucleus (Sylvestre and Cullen 1999a), we conclude that a first order model of eye position (model M3) is the simplest model we can utilize to describe BT neuron discharges during conjugate saccades.

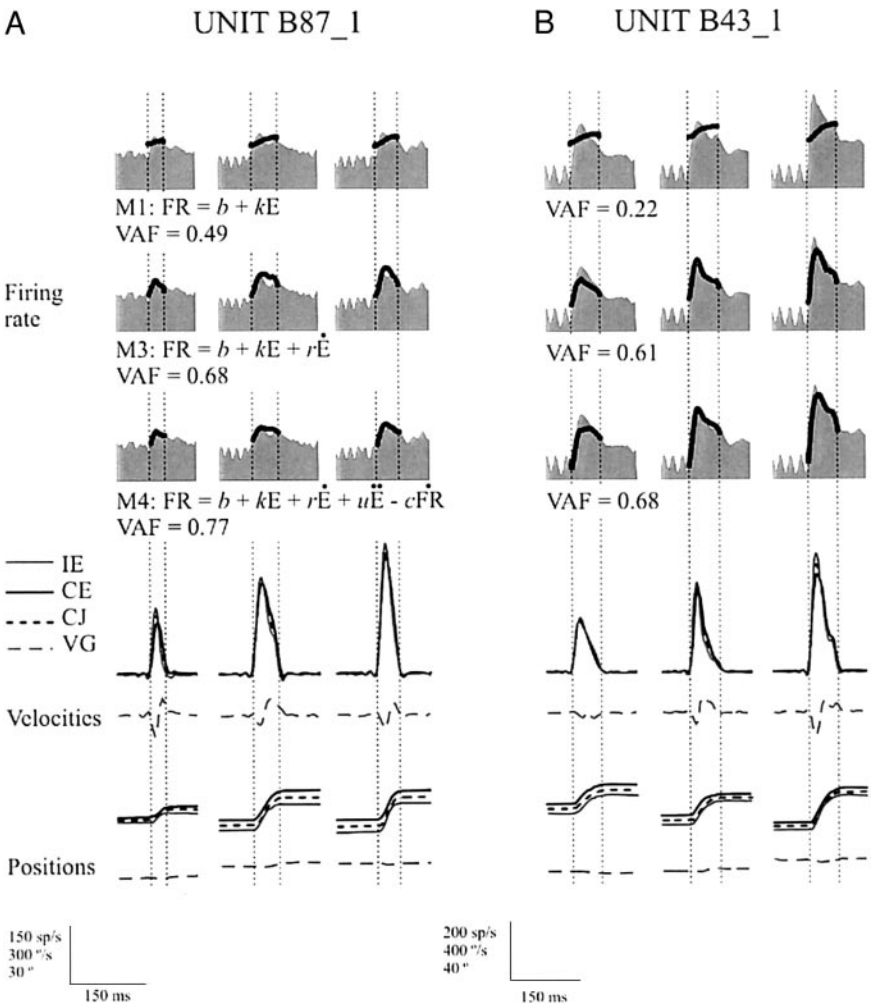


FIG. 4. Two example BT neurons during conjugate saccades. For clarity, the firing rates of *unit B87_1* (*A*) and *unit B43_1* (*B*) were reproduced three times (*top 3 traces*). The thick black curves superimposed on each copy of the firing rates are model fits obtained with models M1, M3, and M4, from top to bottom, respectively. Vertical dotted lines indicate saccade onsets and offsets. Eye velocity and position traces are also shown.

*Disjunctive saccades: example neurons*

The approach that we utilized to characterize the activity of BT neurons during disjunctive saccades was identical to that described in Sylvestre and Cullen (2002). First, for each neuron, we determined whether a model estimated during conjugate saccades (model M3, Table 2) could predict its activity during disjunctive saccades. Second, we estimated the parameters of the following model on the data set of disjunctive saccades collected for that neuron

$$\mathrm{FR}(t) = b_{\mathrm{DS}} + k_{\text{i-DS}}\mathrm{IE}(t - t_{\mathrm{d}}) + k_{\text{c-DS}}\mathrm{CE}(t - t_{\mathrm{d}}) + \cdots$$
$$r_{\text{i-DS}}\dot{\mathrm{IE}}(t - t_{\mathrm{d}}) + r_{\text{c-DS}}\dot{\mathrm{CE}}(t - t_{\mathrm{d}}) \qquad \text{(model Est-all)}$$

where $b_{\mathrm{DS}}$, $k_{\text{i-DS}}$, $k_{\text{c-DS}}$, $r_{\text{i-DS}}$, and $r_{\text{c-DS}}$ are the bias, ipsilateral eye-position, contralateral eye-position, ipsilateral eye-velocity, and contralateral eye-velocity sensitivities of the neuron, respectively (the subscripts DS, i, and c refer to disjunctive saccades, ipsilateral eye, and contralateral eye, respectively), and IE($t$), CE($t$), $\dot{\mathrm{IE}}(t)$ and $\dot{\mathrm{CE}}(t)$ are instantaneous ipsilateral and contralateral eye positions and velocities, respectively. This model is the binocular expansion of model M3. Model M3, rather than model M4, was chosen for this analysis to limit the number of free parameters in model Est-all.

For each parameter in model Est-all, bootstrap confidence intervals (see METHODS) were utilized to reduce the model to its simplest form (reduced model labeled Est-red; can be different for each neuron). This approach was necessary given that some basic assumptions (e.g., normally distributed residuals) inherent to standard statistical tests on linear regression parameters were invalid (see Sylvestre and Cullen 2002 for more details). The bootstrap approach utilized here provided an alternate objective technique to determine which model parameters significantly contributed to the goodness-of-fit of the model to the neuronal firing rates.

*Example monocular BT neuron, unit B87_1*

Figure 5 shows the results of our analysis of disjunctive saccades for *unit B87_1*, the same unit that was shown in Fig. 4*A* during conjugate saccades. The unit's discharge during converging (Fig. 5*A*) and diverging (Fig. 5*B*) saccades are shown. The model predictions, shown in the *top row* (*Pred-CS*) and generated using the parameters of model M3 (Table 2) and the conjugate traces shown at the *bottom* of Fig. 5, clearly could not describe the activity of this neuron during disjunctive saccades. This prediction-based analysis hence suggested that *unit B87_1* did not encode conjugate signals during these movements.

The black model fits in the *second row* of Fig. 5 were obtained by estimating the parameters of model Est-all on the data set of disjunctive saccades gathered for this neuron. In contrast to the model predictions, this estimated model could adequately describe the neuronal activity during both converging and diverging saccades. To determine whether all model parameters were significant, the bootstrap confidence intervals illustrated in Fig. 6 were analyzed. As shown in Fig. 6, both the contralateral eye position ($k_{\text{c-DS}}$) and the contralateral eye velocity terms ($r_{\text{c-DS}}$) in model Est-all had confidence intervals that markedly overlapped with zero (white horizontal bars, Fig. 6). This result indicates that these parameters did not play a significant role in describing the activity of *unit B87_1* during

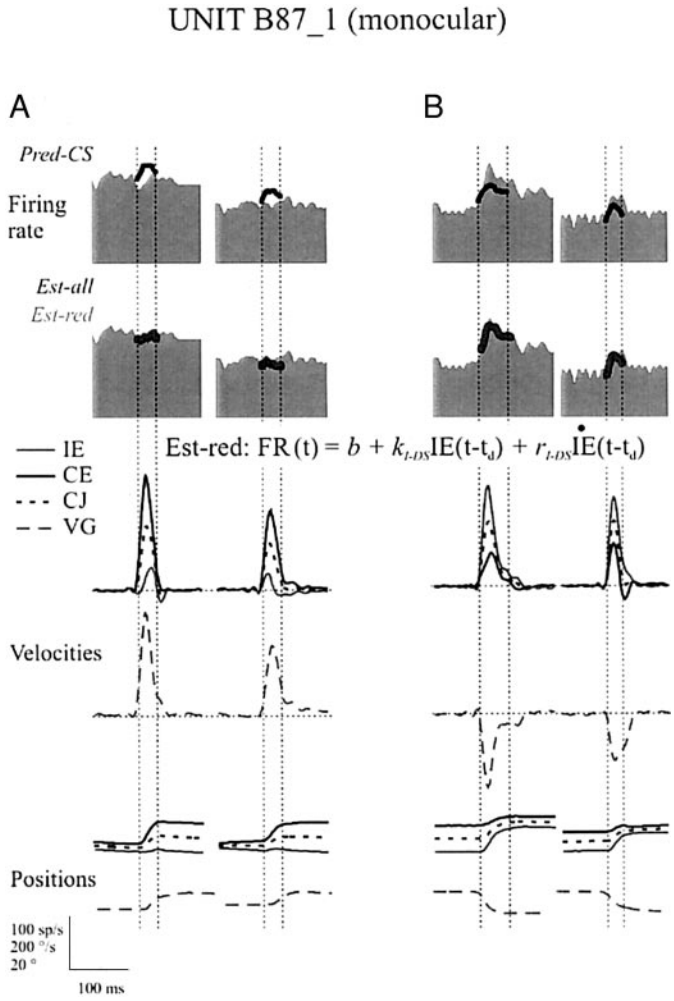


FIG. 5. Example monocular *unit B87_1* during converging (*A*) and diverging (*B*) disjunctive saccades. Note the very different movement dynamics for the ipsilateral and contralateral eyes. *Top*: poor model predictions obtained with Pred-CS. *Second row*: model fits obtained using Est-all (black curve) and Est-red (dark gray curve; equation is also shown). The firing rates were duplicated.

disjunctive saccades (i.e., this unit was monocular with a preference for the ipsilateral eye).

To further validate this conclusion, we removed both terms related to the movements of the contralateral eye from model Est-all and estimated the parameter values of the reduced model [model Est-red, see Fig. 5; for this neuron, $\mathrm{FR}(t) = b_{\mathrm{DS}} + k_{\mathrm{DS}}\mathrm{IE}(t - t_{\mathrm{d}}) + r_{\mathrm{DS}}\dot{\mathrm{IE}}(t - t_{\mathrm{d}})$]. The obtained model fits were quantitatively as good as those obtained with model Est-all (i.e., $\mathrm{VAF}_{\text{Est-all}} = \mathrm{VAF}_{\text{Est-red}} = 0.78$). This is graphically shown in the *second row* of Fig. 5, where the gray model fit (model Est-red) is perfectly superimposed on the black model fit (model Est-all). In summary, both the prediction-based and the estimation / bootstrap-based analyzes indicated that *unit B87_1* did not encode conjugate signals during disjunctive saccades. Rather it solely encoded the position and the velocity of the eye ipsilateral to the recording site.

*Example conjugate BT neuron, unit B43_1*

Figures 7 and 8 show the results of this analysis approach when applied to conjugate *unit B43_1* (also shown in Fig. 4*B*

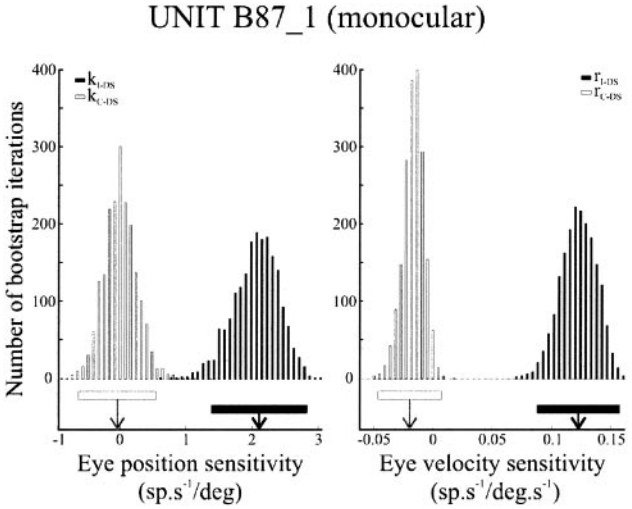


FIG. 6. Bootstrap analysis for monocular *unit B87_1*. *Left*: the results for the eye position sensitivity; *right*: results for the eye velocity sensitivity. The histograms represent the parameter values obtained using Est-all for the ipsilateral (black bars) and contralateral (white bars) eye. The vertical arrows indicate the mean value for each parameter, and the thick horizontal bars are 95% confidence intervals.

during conjugate saccades). One obvious difference with the data shown for *unit B87_1* was that the predictions computed using model M3 were very good for both converging and diverging saccades (Fig. 7, *top*, *A* and *B*, respectively). This observation strongly suggested that *unit B43_1* encoded conjugate eye position and velocity signals during all saccades.

This conclusion was strengthened by the estimation-based analysis. As is shown in Fig. 7, model Est-all provided a very good fit to the data (*2nd row*, black model fits). Furthermore, Fig. 8 clearly shows that for both the eye position ($k_{c\text{-}DS}$ and $k_{i\text{-}DS}$) and the eye velocity ($r_{c\text{-}DS}$ and $r_{i\text{-}DS}$) related terms in model Est-all, the parameter values for the ipsilateral and contralateral eyes were statistically identical (i.e., there was extensive overlap of the confidence intervals). Also note that no term had its confidence interval overlapping with zero (i.e., all terms were significant). These results confirmed that *unit B43_1* encoded conjugate eye-position and -velocity signals. Indeed, when the parameters of model Est-all were replaced by conjugate parameters [model Est-red, see Fig. 7; for this neuron, $FR(t) = b_{DS} + k_{DS}CJ(t - t_d) + r_{DS}\dot{C}J(t - t_d)$], the obtained model fits were identical to those of the full binocular model (*2nd row*, gray model fit, Fig. 7), and so were the VAF values. In summary, our analysis indicated that *unit B43_1* was equally sensitive to the position and velocity of both eyes.

### *Disjunctive saccades: population results*

The population signals carried by BT neurons during disjunctive saccades were quantified using an approach identical to that utilized during disjunctive fixation. For a given neuron, the eye position coefficients estimated in model Est-red for each eye were utilized to calculate a $Ratio_{pos}$ index, and the eye-velocity coefficients to calculate a $Ratio_{vel}$ index. As for fixation, these indexes were used to assign individual neurons to one of the five categories of ocular preferences described in Table 1. With respect to the eye-position sensitivity of BT neurons during disjunctive saccades, most units (70%) encoded

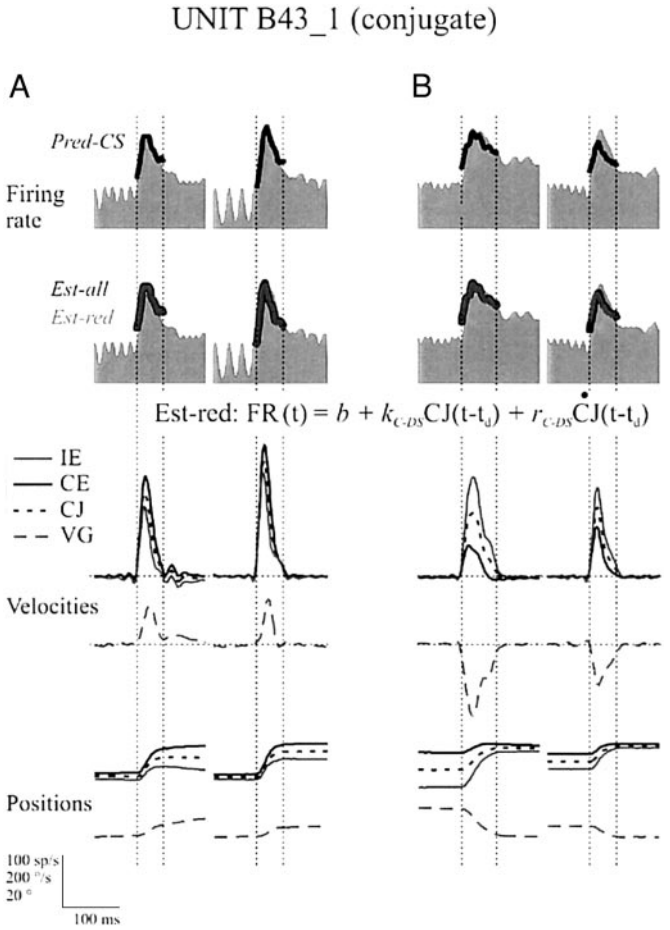


FIG. 7. Example conjugate *unit B87_1* during converging (*A*) and diverging (*B*) disjunctive saccades. The conventions are as in Fig. 5. Note the good predictions obtained with Pred-CS.

the monocular position of one of the eyes (gray bars, Fig. 9*A*). Of these neurons, 50% encoded the position of each eye (pale and dark gray bars, for the ipsilateral and contralateral eyes, respectively). The remaining 30% of BT neurons encoded the conjugate position of the eyes (black bar). Note that in contrast to disjunctive fixation, no neuron unequally encoded binocular signals. A generally similar distribution was observed for the

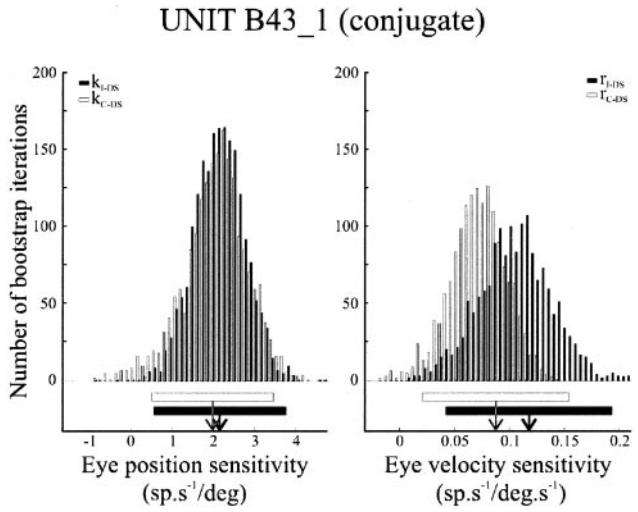


FIG. 8. Bootstrap analysis for conjugate *unit B43_1*.

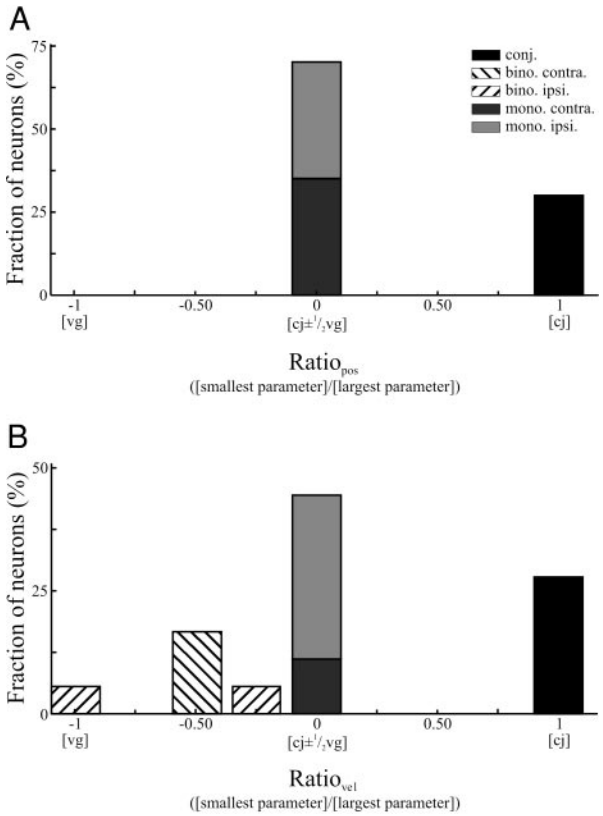


FIG. 9. Distribution of $Ratio_{pos}$ (*A*) and $Ratio_{vel}$ (*B*) during disjunctive saccades for our sample of BT neurons. Conventions are as in Fig. 3.

eye velocity sensitivity of BT neurons (Fig. 9*B*). Overall, many units (35%) encoded the velocity of the ipsilateral eye only, and 20% encoded the conjugate velocity of the eyes. Only 25% of the units unequally encoded binocular signals (stripped bars).

Because each neuron in our sample had a "preferred eye" (defined as the eye that yielded the largest parameter value) for its position and for its velocity sensitivities, we next asked whether these preferred eyes were matched on a neuron-by-neuron basis. To simplify this analysis, the neurons (in the preceding text separated in 5 categories) were regrouped under three general categories: *ipsilateral eye preference* category (grouping the monocular with ipsilateral eye preference and the unequal binocular with ipsilateral eye preference cell types), *contralateral eye preference* category (grouping the monocular with contralateral eye preference and unequal binocular with contralateral eye preference cell types), or *conjugate* category. The fraction of neurons that fell within each of the nine possible permutations among these three categories are illustrated in Fig. 10*A* for the eye-position and -velocity sensitivities estimated during disjunctive saccades. In general, for 55% of the neurons in our sample, there was coherence between their preferred eye for the two sensitivities (Fig. 10*A*, ■). For the remaining neurons that did not exhibit coherence of their preferred eye, no specific pattern could be identified (Fig. 10*A*, ■). Hence, we conclude that a majority of individual BT neurons encoded the position and the velocity of the same eye during disjunctive saccades and that no trend was identified for the neurons that did not exhibit such coherence.

*Disjunctive saccades versus disjunctive fixation*

A similar approach was utilized to compare the "preferred" eye position sensitivities of individual neurons during disjunctive fixation and disjunctive saccades. A neuron's preferred eye for the position sensitivity during disjunctive saccades was the same as during disjunctive fixation for the majority of units (75% coherence; Fig. 10*B*, ■). With respect to the noncoherent units (Fig. 10*B*, ■), they were fairly uniformly distributed. However, it should be noted that even if they preferred the same eye, slightly more units encoded unequal binocular eye position signals during disjunctive fixation (40 vs. 0%), while a comparable number of units encoded the conjugate position of the eyes during both behaviors (20 vs. 20%). Hence, BT neurons generally encoded the position of the same eye during disjunctive fixation and disjunctive saccades but sometimes encoded the position of the nonpreferred eye with different strengths across these behaviors.

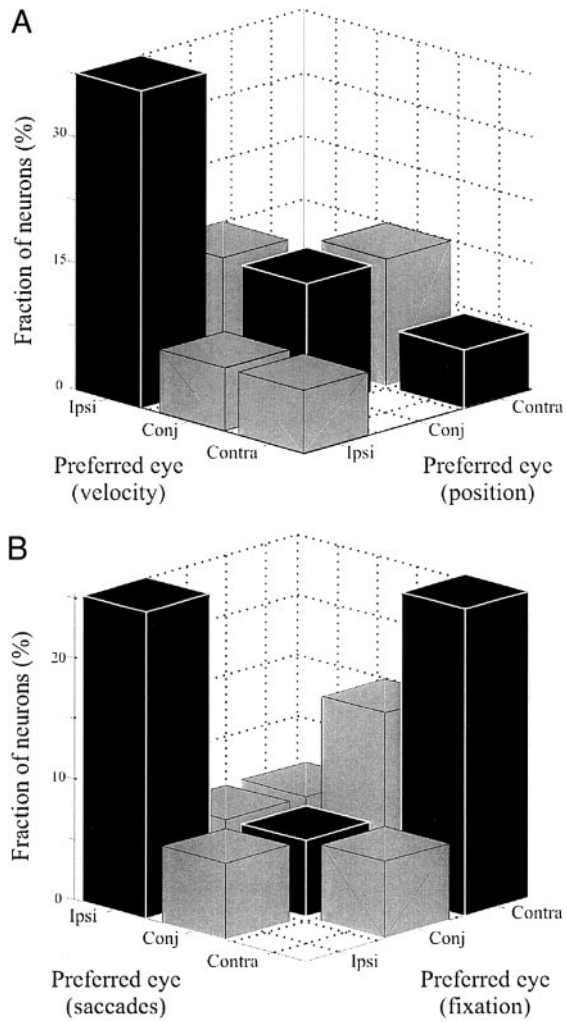


FIG. 10. *A*: coherence of the preferred eyes for the position and velocity sensitivities of BT neurons during disjunctive saccades. Neurons were separated in 3 preferred eye categories (ipsilateral eye, Ipsi; contralateral eye, Contra; or conjugate, Conj) for the position and velocity sensitivities. ■, coherence (i.e., the eye position and the eye velocity preferred eyes of a neuron were the same). *B*: coherence of the preferred eyes for the position sensitivities of BT neurons during disjunctive saccades and disjunctive fixation.

*Disjunctive saccades: alternative analysis model*

Finally, for the sake of completeness, we also analyzed our sample of BT neurons using a model based on conjugate/vergence coordinates

$$FR(t) = b_{DS} + k_{cj\text{-}DS}CJ(t - t_d) + k_{vg\text{-}DS}VG(t - t_d) + \cdots + r_{cj\text{-}DS}\dot{C}J(t - t_d) + r_{vg\text{-}DS}\dot{V}G(t - t_d) \quad \text{(model Est-cv)}$$

where CJ and VG indicate conjugate and vergence parameters, respectively. This additional analysis was necessary because models Est-all and Est-cv are not always equivalent after one or more parameters have been removed and because it has been shown that reliable conjugate/vergence parameter values cannot always be computed from the parameters of model Est-red (Sylvestre and Cullen 2002). Hence, we properly evaluated the parameters of model Est-cv on all the neurons in our sample by independently computing bootstrap confidence intervals for each parameter. Similar to our findings with abducens neurons, we occasionally obtained slightly different results using models Est-all and Est-cv. However, for 75% of the neurons in our sample, the reduced models obtained with model Est-cv provided worse or equivalent goodness-of-fits as those obtained with model Est-all (mean difference in VAF = $-0.04 \pm 0.07$); for the remaining units, the VAF values for the reduced conjugate/vergence-based models were only $0.01 \pm 0.003$ larger than for the reduced binocular models. Hence as for abducens neurons (Sylvestre and Cullen 2002), we conclude that the binocular approach (i.e., using model Est-all) is more appropriate to describe the modulation of BT neurons during disjunctive saccades.

## DISCUSSION

In this report, we have provided the first detailed quantification of the discharge dynamics of BT neurons in the prepositus hypoglossi and medial vestibular nuclei during conjugate saccades and disjunctive saccades. We also compare, on a neuron-by-neuron basis, the discharges recorded during disjunctive saccades and disjunctive fixation. We have shown that these neurons carry both eye-position and -velocity-related signals during conjugate saccades, as well as a smaller (yet important) "slide" term. Further, we have demonstrated that a majority of BT neurons, during disjunctive fixation and disjunctive saccades, preferentially encode the position and velocity of one eye; only few BT neurons equally encoded the movements of both eyes (i.e., had conjugate sensitivities). We argue that BT neurons in the NPH/MVN play an important role in the generation of both the conjugate and the vergence components of disjunctive eye movements.

*Conjugate fixation and general response characteristics*

During conjugate fixation, 90% of the BT neurons in our sample increased their discharges with increasingly ipsilateral eye positions, which compares well with the previous findings (86%) of McFarland and Fuchs (1992). Moreover, the average bias and eye position sensitivities reported here during fixation ($b_{fix} = 66 \pm 48$ spikes/s and $k_{fix} = 3.2 \pm 2.0$ spikes $\cdot$ s$^{-1}$ $\cdot$ °$^{-1}$, respectively), were almost identical to those reported in previous reports [mean $k_{fix} = 3.2 \pm 1.3$ spikes $\cdot$ s$^{-1}$ $\cdot$ °$^{-1}$ (McFarland and Fuchs 1992); mean $k_{fix} = 3.6$ spikes $\cdot$ s$^{-1}$ $\cdot$ °$^{-1}$, (Scudder and Fuchs 1992)]. With respect to conjugate saccadic behavior, 95% of the units described in this report had BT discharge properties, and a single neuron had tonic discharge properties. Previous studies that recorded from nonvestibular neurons in the MVN/NPH have reported slightly lower proportions of BT neurons (73% across NPH/MVN, McFarland and Fuchs 1992; 53% only in MVN, Scudder and Fuchs 1992). This is not surprising, given that for the sake of the analysis utilized in this report, we preferentially recorded from neurons that exhibited significant saccade-related behaviors.

In the monkey, many if not most BT neurons provide significant premotor drives to the abducens nucleus. Both spike-triggered averaging (Scudder and Fuchs 1992) and intracellular recording/staining (McCrea et al. 1987) experiments have identified neurons with BT discharge characteristics that project to the abducens nucleus. In fact, Scudder and Fuchs (1992) have noted that more BT than tonic-only neurons project to the abducens nucleus. Moreover, McFarland and Fuchs (1992) have found that 91% of neurons in the marginal zone, where the highest NPH/MVN projections to the abducens are located (Langer et al. 1986), have burst-tonic discharge characteristics. In this study, we found that, on average, BT neurons had a dynamic lead time that was comparable to that previously reported for premotor medium-lead inhibitory burst neurons ($12.2 \pm 5.3$ vs. $11.8 \pm 2.7$ ms, for BT vs. inhibitory burst neurons) (Cullen and Guitton 1997). Abducens nucleus neurons, on average, had shorter dynamic lead times ($9.4 \pm 1.9$ ms) (Sylvestre and Cullen 1999a). Thus our findings are consistent with previous evidence showing that in the monkey, BT neurons are output neurons of the NI and are therefore premotor neurons.

*Signals encoded by BT neurons during conjugate saccades*

In the monkey, it has been shown that BT neurons discharge bursts of action potentials during saccades whose durations and number of spikes are well correlated with the duration and amplitude of the concurring saccade, respectively (McFarland and Fuchs 1992). Our analysis confirmed and extended these findings by providing the first detailed description of the relationship between the dynamics of the saccadic burst of BT neurons and the ongoing eye movement. We found that, as for ABN neurons (Sylvestre and Cullen 1999a), both the instantaneous eye position *and* instantaneous eye velocity are required to describe BT neuron firing rate dynamics during conjugate saccades (see model M3, Table 2). Moreover, the average parameter values for this model were generally similar for BT neurons and ABN neurons ($b$: $143 \pm 82$ vs. $156 \pm 89$ spikes/s; $k$: $3.9 \pm 2.5$ vs. $4.2 \pm 2.3$ spikes $\cdot$ s$^{-1}$ $\cdot$ °$^{-1}$; $r$: $0.34 \pm 0.31$ vs. $0.42 \pm 0.26$ sp/°; BT vs. ABN neurons, respectively). Interestingly, the largest difference in parameter values was for the eye-velocity-sensitivity parameters, which were on average smaller for BT neurons than ABN neurons. These findings are consistent, during saccades, with BT neurons being a primary source of eye-position-related signals to the abducens nucleus, and with saccadic excitatory burst neurons combining their eye velocity-related drives with those of BT neurons at the level of the abducens nucleus.

We also found that BT neuron discharges carry a "slide" term [i.e., FR($t$), model M4 in Table 2] during saccades that is similar to that of ABN neurons ($0.018 \pm 0.018$ vs. $0.015 \pm$

0.014, BT neurons vs. ABN neurons, respectively) (Sylvestre and Cullen 1999). Postsaccadic slide terms have been described previously for BT neurons (Lopez-Barneo et al. 1982; McFarland and Fuchs 1992). This exponentially decaying term is generally believed to offset the restoring forces of the oculomotor plant following a saccade (Goldstein 1983; Robinson 1964; Sylvestre and Cullen 1999a). Aksay et al. (2001) have further shown that BT neurons, in the goldfish, have the intrinsic properties required to generate a "slide" term. Using in vivo intracellular recordings in alert goldfishes, they have shown that area I neurons (the fish equivalent of NPH/MVN) generate a burst of action potentials that is quickly followed by an exponential decay in firing rate in response to an injected depolarizing pulse. This decay has a time constant (~50 ms) that is similar to that observed on abducens nucleus neurons following saccades (Goldstein 1983; Sylvestre and Cullen 1999a). Taken together, these results are consistent with the proposal that BT neurons contribute to generating the "slide" signal present on ABNs during and following saccades.

### *Signals encoded by BT neurons during disjunctive fixation*

During disjunctive fixation, we have found that only 20% of BT neurons encoded the conjugate position of the eyes (i.e., were equally sensitive to the position of both eyes; Fig. 3), whereas 40% encoded the position of a single eye. To date, the only other study that has quantitatively characterized the activity of BT neurons during disjunctive eye movements is the study by Zhou and King (1996). This study, however, focused on disjunctive smooth pursuit, and there is no a priori reason to assume that BT neurons should generate similar responses during both eye movements. Nevertheless, there are important similarities between their results and ours. For example, during monocular smooth pursuit, most NPH neurons (~70%) are monocular (Zhou and King 1996). The general tendency to observe very few conjugate neurons was therefore common to both samples. However, all the monocular neurons recorded during smooth pursuit preferred the ipsilateral eye, while we recorded equal numbers of neurons encoding the position of each eye during fixation. These latter results are more consistent with the results obtained for the only other premotor neurons studied quantitatively during disjunctive fixation, position-vestibular-pause (PVP) neurons for which 50% encoded the position of either eye (McConville et al. 1994). Further studies will be required to determine whether the results obtained during disjunctive smooth pursuit reflect the likely distinct properties of smooth pursuit premotor pathways or whether they are simply due to sampling biases.

Our result that most BT neurons did not encode conjugate signals during disjunctive fixation suggests a potentially important role for these neurons in generating unequal movements of the eyes (i.e., vergence). To determine the functional relevance of the vergence-related terms carried by BT neurons during disjunctive fixation, we decided to compare the population results obtained for BT neurons during disjunctive fixation to those obtained for ABN neurons during a similar paradigm (Sylvestre and Cullen 2002). This comparison addresses whether BT neurons carry sufficient eye-position-related information to shape the activity of ABN neurons during disjunctive fixation or whether there is a need for additional vergence-related inputs. Strikingly, as shown in Fig. 11*A*, both population distributions were fairly similar. The most notable difference was that fewer BT neurons than ABN neurons

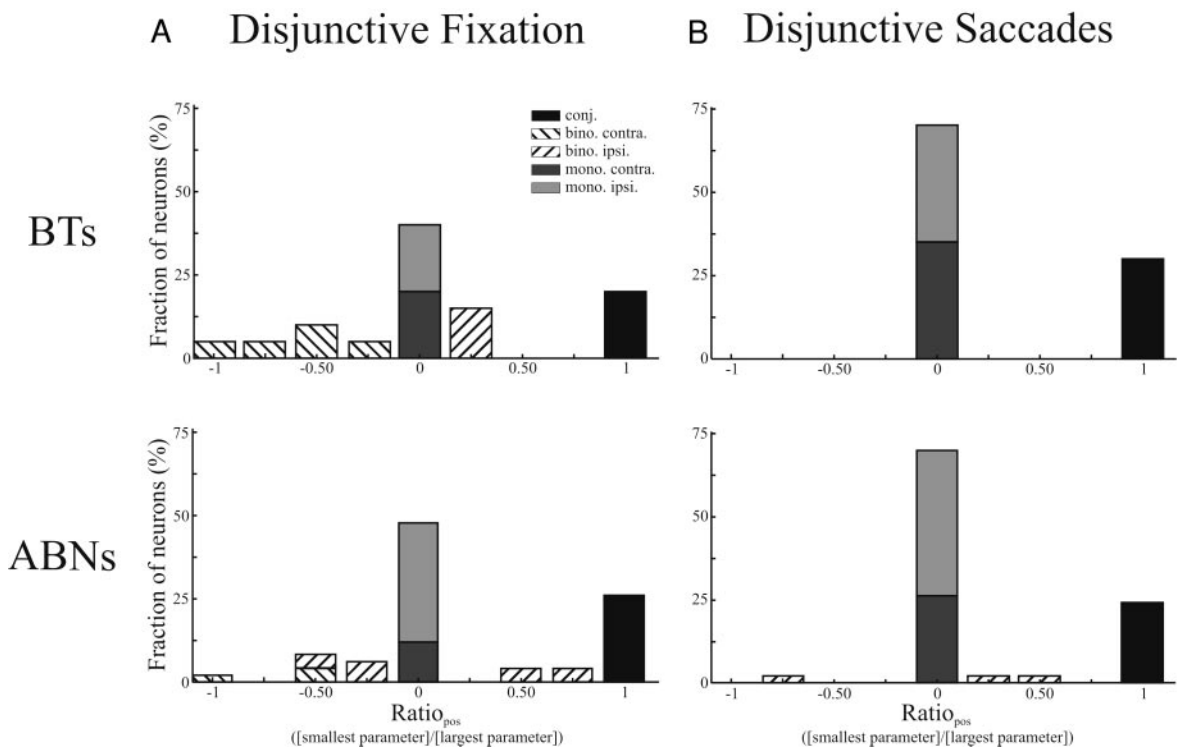


FIG. 11. *A*: comparison of eye-position sensitivities during disjunctive fixation for BT neurons (*top*) and abducens nucleus neurons (ABN) (*bottom*). *B*: comparison of eye-position sensitivities estimated during disjunctive saccades for BT neurons (*top*) and ABN neurons (*bottom*). ABN neuron data modified from Sylvestre and Cullen (2002).

encoded the position of a single eye. One explanation for this small discrepancy is that during disjunctive fixation, other premotor neurons such as PVP neurons were shown to send monocular eye-position-related drives to the abducens nucleus (McConville et al. 1994). Moreover, eye-head neurons, which are also thought to be premotor, have been qualitatively described as preferentially encoding the position of a single eye (Chen-Huang and McCrea 1999). Hence, the summation of the drives carried by BT neurons, PVP neurons, and possibly eye-head neurons, at the level of ABN neurons would account for the signals carried by the latter neurons during disjunctive fixation.

### *Signals encoded by BT neurons during disjunctive saccades*

We have demonstrated that neither of the conceptual frameworks presented in Fig. 1, *A* and *B*, can fully account for the population discharges of BT neurons during disjunctive saccades. Our results revealed that, for both the eye-position and -velocity sensitivities of BT neurons during disjunctive saccades, all units did not encode conjugate eye movements (Fig. 9), which is not consistent with the schema shown in Fig. 1*A*. In addition, most BT neurons we characterized were not purely monocular, in disagreement with the model structure shown in Fig. 1*B*.

When compared with the study of Zhou and King (1996), who recorded the activity of NPH neurons during disjunctive smooth pursuit, our results during disjunctive saccades present a number of similarities. For example, in both paradigms, very few neurons encoded the conjugate position or velocity of the eyes, and many neurons were monocular (see Fig. 9). However, during disjunctive saccades, 50% of monocular BT neurons encoded the position of either eye, whereas 80% encoded the velocity of the ipsilateral eye. These results contrast with those obtained during smooth pursuit, where 100% of monocular NPH neurons encoded the movements of the ipsilateral eye. As suggested in the preceding text, the different results obtained during disjunctive smooth pursuit could reflect distinct properties of the saccadic versus smooth pursuit premotor pathways or alternatively could be due to sampling biases. Furthermore the dynamic analysis/statistical approach utilized here during disjunctive saccades, which was more sensitive than that employed by Zhou and King (1996) during smooth pursuit, could also potentially explain the different results obtained across studies. Nevertheless, the general trends observed across experiments, eye movement types and analysis approaches suggest that the rules for controlling disjunctive eye movements are fairly uniform at the brain stem level.

Our experimental results also allowed us to test the predictions of more recent model structures (Cova and Galiana 1994–1996; Sylvestre et al. 2002; also see King and Zhou 2000, 2002). In these model structure, BT neurons should encode sufficient conjugate and vergence signals such that, as a population, they can shape the discharges of ABN neurons. Hence, we tested this model's predictions by comparing the population results obtained for BT neurons and ABN neurons during disjunctive saccades (Sylvestre and Cullen 2002). With respect to the eye-position sensitivities of these neurons during disjunctive saccades, the situation is somewhat simplified relative to disjunctive fixation (see following text) because most PVP neurons stop firing or have markedly reduced firing rates during saccades (Cullen and McCrea 1993; Fuchs and Kimm 1975; Keller and Daniels 1975; Keller and Kamath 1975; Roy and Cullen 1998, 2002; Scudder and Fuchs 1992), and so do 55% of eye-head neurons (Roy and Cullen 2003). Consequently, during disjunctive saccades, BT neurons provide most of the eye-position-related signals carried by ABN neurons, which facilitates the direct comparison between the population properties of premotor and motor neurons.

Figure 11*B* shows that indeed during disjunctive saccades, the distribution of $\text{Ratio}_{\text{pos}}$ for BT and ABN neurons are almost identical. Accordingly, with respect to the eye-position-related premotor signals generated during disjunctive eye movements, we propose that BT neurons in the NPH/MVN, together with PVP neurons and possibly eye-head neurons during fixation, encode sufficient binocular information to account for the eye-position sensitivities recorded in ABN neurons during similar paradigms. This result is crucial as it minimizes the importance of yet undetermined projections from midbrain near-response neurons and vergence velocity neurons (Mays 1984; Mays and Gamlin 1995a,b; Zhang et al. 1991, 1992), or from any other neurons that solely encode vergence, to the abducens nucleus.

The eye-velocity-related modulations encoded by BT neurons during disjunctive saccades also support the predictions made by these models. As for the eye position sensitivities, only a small fraction of BT neurons (20%) encoded the conjugate velocity of the eyes, while almost half (45%) of BT units encoded the velocity of a single eye. The distribution of $\text{Ratio}_{\text{vel}}$ that we obtained for BT neurons was also very similar to that of ABN neurons (compare Fig. 9*B* in the present report to Fig. 8A in Sylvestre and Cullen 2002). Hence, our results are consistent with BT neurons carrying conjugate and vergence velocity-related drives that are highly appropriate to shape the activity of ABN neurons during disjunctive saccades. We propose that the small differences in the eye-velocity-related distributions of BT and ABN neurons can be accounted for by saccadic burst neurons because they also encode monocular velocity signals (i.e., combinations of conjugate and vergence signals) during disjunctive saccades (Sylvestre and Cullen 1999b; Zhou and King 1998). The 45% of eye-head neurons that burst during saccades (Roy and Cullen 2003) could also contribute to these differences, although their discharge patterns during disjunctive saccades remain unexplored.

### *Implications for the upstream control of saccades*

The signals carried by BT neurons during disjunctive saccades and fixation could be generated by conjugate and vergence velocity-related signals originating from separate sources converging on BT neurons, where they are integrated. However, recent experimental evidence suggests that conjugate and vergence signals are merged upstream to BT neurons, at the level of saccadic burst neurons (Sylvestre and Cullen 1999b; Zhou and King 1998) and possibly even at the level of the superior colliculi. There is indeed experimental evidence suggesting that this latter structure is involved in the control of vergence eye movements. First, electrical stimulation in the superior colliculus perturb both the conjugate and the vergence component of disjunctive saccades (Chaturvedi and VanGisbergen 2000, 1999). Second, known inputs to the superior colliculi were shown to be modulated by depth-related stimuli

such as disparity (frontal eye field: Ferraina et al. 2000; lateral intraparietal area (LIP): Gnadt and Mays 1995), suggesting that required conjugate and vergence demands for a particular saccade are computed, at least in these upstream cortical structures, by using information from both retinas. Finally, it was shown that most neurons' firing rates in the superior colliculus are modulated differently during conjugate and disjunctive saccades (Walton 2002). However, the complex spatiotemporal encoding of signals in this midbrain structure has not allowed for firm conclusions to be made on the coordinate frame utilized by these neurons. More single-unit experiments will be required in the superior colliculus and upstream structures to determine the site(s) at which conjugate and vergence commands are computed and then merged.

### *Implications for the downstream control of saccades*

Although we have found that BT neurons have appropriate discharges to shape the discharges of ABN neurons, we also observed that these signals were not perfectly optimized. For instance, as shown in Fig. 11, a number of BT and ABN neurons encoded, to various extents, the movements of the "wrong" eye (e.g., the contralateral eye for a motoneuron). In the case of abducens internuclear neurons, this "problem" can be corrected at the level of the oculomotor nucleus through projections from near-response neurons (Gamlin et al. 1989). However, in the case of abducens motoneurons, these apparently inadequate signals raise important questions. Because these motoneurons create the contraction of the lateral rectus of the ipsilateral eye, which in turn generates the movements of that eye during abducting conjugate and disjunctive saccades, their discharges should reflect the motion of that eye. We have previously shown that during conjugate saccades and eye-head gaze shifts, this relationship is indeed respected (Cullen et al. 2001).

To explain how this relationship is respected during disjunctive eye movements requires considering different mechanisms. One possible mechanism that could account for our results is that co-contraction of the medial rectus, during disjunctive eye movements, contributes to offsetting the contralateral eye-related drives that some motoneurons carry. However, we have previously argued that this mechanism would accentuate the mismatch between the motoneuron discharges and the eye movement rather than improving it (Sylvestre and Cullen 2002). Another possible mechanism is that the connections between abducens motoneurons and lateral rectus muscle fibers can have a broad range of neuromuscular properties (e.g., nonuniform synaptic weights, different muscle fiber types, motor unit specialization) that are unmasked only when the movements of the two eyes are dissociated as during disjunctive eye movements. Hence motoneurons that encode the movements of the contralateral eye could have weaker weights and vice versa for neurons that encode the movements of the ipsilateral eye (Sylvestre and Cullen 2002). This proposed mechanism would also apply, of course, during conjugate saccades. However, because both eyes rotate with virtually identical dynamics during conjugate saccades, this additional level of organization within the extra-ocular muscles would not be apparent.

Recent experiments by Miller and colleagues (2002) have provided further experimental evidence to support this hypothesis. Using implanted miniature muscle force transducers, they have shown that if the position of one of the eyes is kept constant, while the position of the other eye is changed by going from diverged to converged states, the forces generated by both the lateral and medial recti in the immobile eye remain relatively constant. In contrast to this rather intuitive result, it was shown that as a population, abducens neurons are more active in the converged state (Mays and Porter 1984). Hence, there is once again an apparent dissociation between the population drives of abducens motoneurons and lateral muscle force that is revealed during disjunctive, but not during conjugate, eye movements. On the one hand, the patterns of activity of abducens neurons are easily explained by current available data: if we consider those neurons that encode the position of the contralateral eye, they would be more excited during symmetric convergence than during conjugate fixation because the contralateral eye would be deviated toward the neuron's ON direction only in the former case (Sylvestre and Cullen 2002). On the other hand, the mismatch of neural drives and muscle forces can only be accounted for by yet undetermined local mechanisms at the level of the extraocular muscles.

A hypothetical explanation for this additional level of complexity may be offered based on an evolutionary argument. It could be argued that the brain stem saccadic circuitry, which originally was designed to generate rapid conjugate eye movements, was modified through evolution to also generate vergence eye movements. However, this evolution was limited to protect the accuracy of the conjugate component of saccades at the expense of coarser vergence components. Consequently, neurons in this saccadic pathway (and their target neurons in the abducens nucleus) would encode some vergence-related signals but not enough to perfectly compute the movements of a single eye. These "imperfectly" optimized drives would be compensated for at the muscle level. An interesting prediction of this proposal is that vergence eye movements should be less efficient than saccadic eye movements especially during disjunctive saccades. Indeed, there is evidence that for disjunctive saccades with large vergence demands, the vergence shift is often not fully completed during the saccadic phase and requires slower postsaccadic vergence eye movements to complete the vergence shift (human: Collewijn et al. 1995, 1997; Enright 1984; Erkelens et al. 1989; Kenyon et al. 1980; Ono et al. 1978; Oohira 1993; Zee et al. 1992; monkey: Maxwell and King 1992). This fine tuning of the vergence shift is likely completed under visual feedback by the circuitry that generates slower "pure" vergence shifts (e.g., Mays 1984; Mays and Gamlin 1995a,b; Zhang et al. 1991, 1992).

### *General conclusions*

The results presented in this report have broad implications for our understanding of disjunctive eye movements. We have shown that during disjunctive saccades, BT neurons in the NPH/MVN, which were formerly assumed to drive conjugate eye movements only, also contribute to driving vergence eye movements. Specifically, we have shown that the drives carried by these neurons during disjunctive saccades, and also during disjunctive fixation, are appropriate to shape the discharges of their target neurons in the abducens nucleus without the use of an additional purely vergence-related drive. These results sug-

gest that the control of conjugate and vergence eye movements is highly integrated in the brain stem saccadic circuitries.

We are thankful to S. Sadeghi Ghandehari and M. McCluskey for comments on the manuscript. We also thank W. Kucharski, E. Moreau, and J. Knowles for great technical support.

## DISCLOSURES

This study was supported by the Canadian Institutes of Health Research, the Natural Science and Engineering Research Council of Canada, and the Fonds de la Recherche en Santé du Québec.

## REFERENCES

**Aksay E, Gamkrelidze G, Seung HS, Baker R, and Tank DW.** In vivo intracellular recording and perturbation of persistent activity in a neural integrator. *Nat Neurosci* 4: 184–193, 2001.

**Arnold DB, Robinson DA, and Leigh RJ.** Nystagmus induced by pharmacological inactivation of the brain stem ocular motor integrator in monkey. *Vision Res* 39: 4286–4295, 1999.

**Brodal A.** The perihypoglossal nuclei in the macaque monkey and the chimpanzee. *J Comp Neurol* 218: 257–269, 1983.

**Carpenter J and Bithell J.** Bootstrap confidence intervals: when, which, what? A practical guide for medical statisticians. *Statist Med* 19: 1141–1164, 2000.

**Chaturvedi V and Van Gisbergen JAM.** Perturbation of combined saccade-vergence movements by microstimulation in monkey superior colliculus. *J Neurophysiol* 81: 2279–2296, 1999.

**Chaturvedi V and Van Gisbergen JAM.** Stimulation in the rostral pole of monkey superior colliculus: effects on vergence eye movements. *Exp Brain Res* 132: 72–78, 2000.

**Chen-Huang C and McCrea RA.** Effects of viewing distance on the responses of horizontal canal-related secondary vestibular neurons during angular head rotation. *J Neurophysiol* 81: 2517–2537, 1999.

**Clendaniel RA and Mays LE.** Characteristics of antidromically identified oculomotor internuclear neurons during vergence and versional eye movements. *J Neurophysiol* 71: 1111–1127, 1994.

**Collewijn H, Erkelens CJ, and Steinman RM.** Voluntary binocular gaze-shifts in the plane of regard: dynamics of version and vergence. *Vision Res* 35: 3335–3358, 1995.

**Collewijn H, Erkelens CJ, and Steinman RM.** Trajectories of the human binocular fixation point during conjugate and non-conjugate gaze-shifts. *Vision Res* 37: 1049–1069, 1997.

**Cova A and Galiana HL.** Providing distinct vergence and version dynamics in a bilateral oculomotor network. *Vision Res* 35: 3359–3371, 1995.

**Cova A and Galiana HL.** A bilateral model integrating vergence and the vestibulo-ocular reflex. *Exp Brain Res* 107: 435–452, 1996.

**Cova AC and Galiana HL.** A bilateral model of vergence nystagmus. *Proc 16th IEEE EMBS*, Baltimore, MD, 1994, pp. 263–264.

**Cullen KE, Chen-Huang C, and McCrea RA.** Firing behavior of brain stem neurons during voluntary cancellation of the horizontal vestibuloocular reflex. II. Eye movement related neurons. *J Neurophysiol* 70: 844–856, 1993.

**Cullen KE and Guitton D.** Analysis of primate IBN spike trains using system identification techniques. I. Relationship to eye movement dynamics during head-fixed saccades. *J Neurophysiol* 78: 3259–3282, 1997.

**Cullen KE, Galiana HL, and Sylvestre PA.** Comparing extraocular motoneuron discharges during head-restrained saccades and head-unrestrained gaze shifts. *J Neurophysiol* 83: 630–637, 2001.

**Cullen KE and McCrea RA.** Firing behavior of brain stem neurons during voluntary cancellation of the horizontal vestibuoocular reflex. I. Secondary vestibular neurons. *J Neurophysiol* 70: 828–843, 1993.

**Cullen KE, Rey CD, Guitton D, and Galiana HL.** The use of system identification techniques in the analysis of oculomotor burst neuron spike train dynamics. *J Comput Neurosci* 3: 347–368, 1996.

**Delgado-Garcia JM, Vidal PP, Gomez C, and Berthoz A.** A neurophysiological study of prepositus hypoglossi neurons projecting to oculomotor and preoculomotor nuclei in the alert cat. *Neuroscience* 29: 291–307, 1989.

**Enright JT.** Changes in vergence mediated by saccades. *J Physiol* 350: 9–31, 1984.

**Erkelens CJ Steinman RM, and Collewijn H.** Ocular vergence under natural conditions. II. Gaze shifts between real targets differing in distance and direction. *Proc R Soc Lond* 236: 441–465, 1989.

**Escudero M, De La Cruz RR, and Delgado-Garcia JM.** A physiological study of vestibular and prepositus hypoglossi neurones projecting to the abducens nucleus in the alert cat. *J Physiol* 458: 539–560, 1992.

**Ferraina S, Pare M, and Wurtz RH.** Disparity sensitivity of frontal eye field neurons. *J Neurophysiol* 83: 625–629, 2000.

**Fuchs AF and Kimm J.** Unit activity in vestibular nucleus of the alert monkey during horizontal angular acceleration and eye movement. *J Neurophysiol* 38: 1140–1161, 1975.

**Fuchs AF and Robinson DA.** A method for measuring horizontal and vertical eye movements in the monkey. *J Physiol* 191: 609–631, 1966.

**Fukushima K, Kaneko CR, and Fuchs AF.** The neuronal substrate of integration in the oculomotor system. *Prog Neurobiol* 39: 609–639, 1992.

**Gamlin PDR.** Subcortical neural circuits for ocular accommodation and vergence in primates. *Ophthalmic Physiol Opt* 19: 81–89, 1999.

**Gamlin PDR, Gnadt JW, and Mays LE.** Abducens internuclear neurons carry an inappropriate signal for ocular convergence. *J Neurophysiol* 62: 70–81, 1989.

**Gamlin PDR and Mays LE.** Dynamic properties of medial rectus motoneurons during vergence eye movements. *J Neurophysiol* 67: 64–74, 1992.

**Gnadt JW and Mays LE.** Neurons in monkey parietal area LIP are tuned for eye-movement parameters in three-dimensional space. *J Neurophysiol* 73: 280–297, 1995.

**Goldstein HP.** *The Neural Encoding of Saccades in the Rhesus Monkey* (PhD thesis). Baltimore, MD: Johns Hopkins University, 1983.

**Hayes AV, Richmond BJ, and Optican LM.** A UNIX-based multiple process system for real-time data acquisition and control. *WESCON Conf Proc* 2: 1–10, 1982.

**Helmholtz JA.** *Treatise on Physiological Optics.* New York: Dover, 1910.

**Hering E.** *Lehre vom Binokularen Sehen. (The Theory of Binocular Vision) (1868),* edited by Bridgeman B and Stark L. New York: Plenum, 1977.

**Judge SJ and Cumming BG.** Neurons in monkey midbrain with activity related to vergence eye movement and accomodation. *J Neurophysiol* 55: 915–930, 1986.

**Judge SJ, Richmond BJ and Chu FC.** Implantation of magnetic search coils for measurement of eye position: an improved method. *Vision Res.* 20: 535–538, 1980.

**Kaneko CR.** Eye movement deficits after ibotenic acid lesions of the nucleus prepositus hypoglossi in monkeys. I. Saccades and fixation. *J Neurophysiol* 78: 1753–1768, 1997.

**Kaneko CR.** Eye movement deficits following ibotenic acid lesions of the nucleus prepositus hypoglossi in monkeys. II. Pursuit, vestibular, and optokinetic responses. *J Neurophysiol* 81: 668–681, 1999.

**Keller EL.** Accomodative vergence in the alert monkey. Motor unit analysis. *Vision Res* 13: 1565–1575, 1973.

**Keller EL and Daniels PD.** Oculomotor related interaction of vestibular and visual stimulation in vestibular nucleus cells in alert monkey. *Exp Neurol* 46: 187–198, 1975.

**Keller EL and Kamath BY.** Characteristics of head rotation and eye movement-related neurons in alert monkey vestibular nucleus. *Brain Res* 100: 182–187, 1975.

**Keller EL and Robinson DA.** Abducens unit behavior in the monkey during vergence movements. *Vision Res* 12: 369–382, 1972.

**Kenyon RV, Ciuffreda KJ, and Stark L.** Unequal saccades during vergence. *Am J Opt Physiol Opt* 57: 586–594, 1980.

**King WM, Zhou W, Tomlinson RD, McConville KM, Page WK, Paige GD, and Maxwell JS.** Eye position signals in the abducens and oculomotor nuclei of monkeys during ocular convergence. *J Vestib Res* 4: 401–408, 1994.

**King WM and Zhou W.** New ideas about binocular coordination of eye movements: is there a chameleon in the primate family tree?. *New Anat* 261: 153–161, 2000.

**King WM and Zhou W.** Neural basis of disjunctive eye movements. *Ann. N.Y. Acad. Sci* 956: 273–283, 2002.

**Langer T, Kaneko CR, Scudder CA, and Fuchs AF.** Afferents to the abducens nucleus in the monkey and cat. *J Comp Neurol* 245: 379–400, 1986.

**Lopez-Barneo J, Darlot C, Berthoz A, and Baker R.** Neuronal activity in prepositus nucleus correlated with eye movement in the alert cat. *J Neurophysiol* 47: 329–352, 1982.

**Maxwell JS and King WM.** Dynamics and efficacy of saccade-facilitated vergence eye movements in monkeys. *J Neurophysiol* 68: 1248–1260, 1992.

**Mays LE.** Neural control of vergence eye movements: convergence and divergence neurons in midbrain. *J Neurophysiol* 51: 1091–1108, 1984.

**Mays L.** Has Hering been hooked? *Nat Med* 4: 889–890, 1998.

**Mays LE and Gamlin PDR.** Neuronal circuitry controlling the near response. *Curr Opin Neurobiol* 5: 763–768, 1995a.

**Mays LE and Gamlin PDR.** A neural mechanism subserving saccade-vergence interactions. In: *Eye Movement Research: Mechanisms, Processes and Applications,* edited by Findlay J, Walker R, and Kentridge RW. Amsterdam: Elsevier, p. 215–223, 1995b.

**Mays LE and Porter JD.** Neural control of vergence eye movements: activity of abducens and oculomotor neurons. *J Neurophysiol* 52: 743–761, 1984.

**Mays LE, Porter JD, Gamlin PDR, and Tello CA.** Neural control of vergence eye movements: neurons encoding vergence velocity. *J Neurophysiol* 56: 1007–1021, 1986.

**McConville K, Tomlinson RD, King WM, Paige G, and Na E-Q.** Eye position signals in the vestibular nuclei: consequences for models of integrator function. *J Vestib Res* 4: 391–400, 1994.

**McCrea RA.** Neuroanatomy of the oculomotor system. The nucleus prepositus. *Rev Oculomot Res* 2: 203–223, 1988.

**McCrea RA, Strassman A, May E, and Highstein SM.** Anatomical and physiological characteristics of vestibular neurons mediating the horizontal vestibulo-ocular reflex of the squirrel monkey. *J Comp Neurol* 264: 547–570, 1987.

**McFarland JL and Fuchs AF.** Discharge patterns in nucleus prepositus hypoglossi and adjacent medial vestibular nucleus during horizontal eye movement in behaving macaques. *J Neurophysiol* 68: 319–332, 1992.

**Mettens P, Godaux E, Cheron G, and Galiana HL.** Effect of muscimol microinjections into the prepositus hypoglossi and the medial vestibular nuclei on cat eye movements. *J Neurophysiol* 72: 785–802, 1994.

**Miller JM, Bockish CJ, and Pavlovski DS.** Missing lateral rectus force and absence of medial rectus co-contraction in ocular convergence. *J Neurophysiol* 87: 2421–2433, 2002.

**Moschovakis AK.** The neural integrators of the mammalian saccadic system. *Front Biosci* 15: D552–D577, 1997.

**Ono H, Nakamizo S, and Steinbach MJ.** Nonadditivity of vergence and saccadic eye movement. *Vision Res* 18: 735–739, 1978.

**Oohira A.** Vergence eye movements facilitated by saccades. *Jpn J Ophthalmol* 37: 400–413, 1993.

**Press WH, Teukolsky SA, Vetterling WT and Flannery BP.** *Numerical recipes in C. The art of scientific computing* (2nd ed.). New York: Cambridge, 1997, p. 689–693.

**Richmond BJ, Optican LM, Podell M, and Spitzer H.** Temporal encoding of two-dimensional patterns by single units in primate inferior temporal cortex. I. Response characteristics. *J Neurophysiol* 57: 132–146, 1987.

**Robinson DA.** The mechanics of human saccadic eye movement. *J Physiol* 174: 245–264, 1964.

**Robinson DA.** Oculomotor unit behavior in the monkey. *J Neurophysiol* 33: 393–404, 1970.

**Robinson DA. and Keller EL.** The behaviour of eye movement motoneurons in the alert monkey. *Bibl Ophthalmol* 82: 7–16, 1972.

**Roy JE and Cullen KE.** A neural correlate for vestibulo-ocular reflex suppression during voluntary eye-head gaze shifts. *Nat Neurosci* 1: 404–410, 1998.

**Roy JE and Cullen KE.** Vestibuloocular reflex signal modulation during voluntary and passive head movements. *J Neurophysiol* 87: 2337–2357, 2002.

**Roy JE and Cullen KE.** Brain stem pursuit pathways: dissociating visual, vestibular, and proprioceptive inputs during combined eye-head gaze tracking. *J Neurophysiol* 90: 271–290, 2003.

**Schwartz G.** Estimating the dimension of a model. *Ann Statist* 6: 461–464, 1978.

**Scudder CA and Fuchs AF.** Physiological and behavioral identification of vestibular nucleus neurons mediating the horizontal vestibuloocular reflex in trained rhesus monkeys. *J Neurophysiol* 68: 244–264, 1992.

**Scudder CA, Kaneko CRS, and Fuchs AF.** The brain stem burst generator for saccadic eye movements. A modern synthesis. *Exp Brain Res* 142: 439–462, 2002.

**Sokal RR and Rohlf FJ.** *Biometry. The Principles and Practice of Statistics in Biological Research* (3rd ed.). New York: Freeman, 1995, p. 820–825.

**Sylvestre PA and Cullen KE.** Quantitative analysis of abducens neuron discharge dynamics during saccadic and slow eye movements. *J Neurophysiol* 82: 2612–2632, 1999a.

**Sylvestre PA and Cullen KE.** Monocularly tuned discharge dynamics of abducens and brain stem inhibitor burst neurons during disjunctive saccades. *Soc Neurosci Abstr* 25, 1652, 1999b.

**Sylvestre PA and Cullen KE.** Dynamics of abducens nucleus neuron discharges during disjunctive saccades. *J Neurophysiol* 88: 3452–3468, 2002.

**Sylvestre PA, Galiana HL, and Cullen KE.** Conjugate and vergence oscillations during saccades and gaze shifts: implications for integrated control of binocular motion. *J Neurophysiol* 87: 257–272, 2002.

**Van Gisbergen JAM, Robinson DA, and Gielen S.** A quantitative analysis of the generation of saccadic eye movements by burst neurons. *J Neurophysiol* 45: 417–442, 1981.

**Walton MMG.** *The Role of the Superior Colliculus in Saccade-Vergence Interactions* (PhD thesis). Birmingham, AL: The University of Alabama, 2002.

**Zee DS, Fitzgibbon EJ and Optican LM.** Saccade-vergence interactions in humans. *J Neurophysiol* 68: 1624–1641, 1992.

**Zhang Y, Gamlin PDR, and Mays LE.** Antidromic identification of midbrain near response cells projecting to the oculomotor nucleus. *Exp Brain Res* 84: 525–528, 1991.

**Zhang Y, May, LE and Gamlin PDR.** Characteristics of near response cells projecting to the oculomotor nucleus. *J Neurophysiol* 67: 944–960, 1992.

**Zhou W and King WM.** Ocular selectivity of units in oculomotor pathways. *Ann NY Acad Sci* 781: 724–728, 1996.

**Zhou W and King WM.** Premotor commands encode monocular eye movements. *Nature* 393: 692–695, 1998.